Nuclear Physics B355 (1991) 511–548
North-Holland

A $U(1)_L \otimes U(1)_R$ SYMMETRIC YUKAWA MODEL IN THE PHASE WITH SPONTANEOUSLY BROKEN SYMMETRY

L. LIN, I. MONTVAY and H. WITTIG

Deutsches Elektronen-Synchrotron DESY, Notkestrasse 85, D-2000 Hamburg 52, Germany

G. MÜNSTER*

II. Institut für Theoretische Physik der Universität Hamburg, Luruper Chaussee 149, D-2000 Hamburg 50, Germany

Received 5 September 1990
(Revised 2 November 1990)

The lattice regularized $U(1)_L \otimes U(1)_R$ symmetric scalar-fermion model with a mirror pair of fermion fields is investigated in the phase with spontaneously broken symmetry. The reflection positivity condition, ensuring unitarity in Minkowski space, is proven in this lattice formulation in a wide range of bare parameters. Numerical Monte Carlo calculations with dynamical fermions are performed on $4^3 \times 8$, $4^3 \times 16$ and $6^3 \times 16$ lattices at moderately strong bare Yukawa couplings and at very small and infinite bare quartic scalar coupling. It is shown that not only the lattice fermion doublers but also the mirror fermion can be made heavy, and therefore the light fermion spectrum is "chiral" as in the standard model. The "vacuum stability" bound on the Higgs-boson mass is discussed in lattice perturbation theory and non-perturbatively. It implies that for heavy mirror fermions the Higgs-boson mass has to be close to the non-perturbative upper limit.

1. Introduction

Recently the experimental lower limits on the masses of the Higgs boson and top quark increased considerably [1, 2]. Since large masses are due to strong couplings to the Higgs field, the more likely existence of a strongly interacting Higgs sector

* Present address: Institut für Theoretische Physik I, Universität Münster, Wilhelm-Klemm-Strasse 9, D-4400 Münster, Germany.

makes the non-perturbative investigations of the scalar-fermion sector of the standard model more and more important. At present the numerical simulation of the complete Higgs–Yukawa sector of the standard model would certainly be premature, if not impossible. One can, however, expect that at least the qualitative features of the non-perturbative behaviour can be discovered in simple prototype models. In fact, recently several groups stated a series of non-perturbative investigations of simple lattice scalar-fermion models [3–8]. (For further references see the review in ref. [9].)

In previous papers we started the non-perturbative study of a $U(1)_L \otimes U(1)_R$ symmetric Yukawa model with a complex scalar field and a mirror pair of fermion fields [10, 11]. Both these papers are dealing with the symmetric phase: in ref. [10] the limit of infinitely heavy fermions is studied, whereas in ref. [11] numerical simulations on lattices with different sizes are performed and compared to the results of lattice perturbation theory and hopping parameter expansion. In the present paper we start the investigation of the phase with spontaneously broken symmetry in this $U(1)_L \otimes U(1)_R$ symmetric model. In fact, the standard model is defined in the broken phase, and therefore the primary interest is in this phase. The study of the symmetric phase is only a preparation and a supplement to the study of the broken phase. The $U(1)_L \otimes U(1)_R$ model has many important qualitative features in common with the $SU(2)_L \otimes SU(2)_R$ model [12] and with the $SU(2)_L \otimes U(1)_Y$ symmetric model for mirror pairs of standard fermion families [13]. In particular, due to the breaking of a continuous global symmetry there is a massless Goldstone boson in the broken phase. From the point of view of axial anomalies this model is particularly interesting, because a U(1) axial symmetry can be anomalous (unlike SU(2)). As far as numerical simulations are concerned, the smaller number of degrees of freedom saves computer time. In the same way as in refs. [10, 11], neither the full $U(1)_L \otimes U(1)_R$ symmetry nor its $U(1)_L$ subgroup are gauged here. The gauge interactions are left for later studies. Similarly to ref. [11], the numerical simulations are performed here by starting from the vicinity of the gaussian fixed point at zero bare couplings where the perturbative standard model is usually defined. The bare Yukawa couplings are increased only to moderately strong values but the bare quartic scalar coupling is allowed to become infinitely strong. Very strong bare Yukawa couplings will be considered in a subsequent work [14].

The main results in ref. [11] are:

(i) The lattice fermion doublers (there are 30 of them in this formulation) can be kept heavy;

(ii) The renormalization of the Yukawa couplings is rather weak, therefore the Callan–Symanzik β-functions are small, their qualitative behaviour is closer to the two-loop than to the one-loop approximation;

(iii) The measured values of the renormalized Yukawa couplings are surprisingly large, at least twice the value of the tree unitarity bound;

(iv) For moderately strong bare Yukawa couplings the dependence of physical quantities on the bare quartic coupling is very weak.

These findings have qualitative consequences also for the broken phase which have to be taken into account in the strategy of the numerical simulations. Due to spontaneous symmetry breaking the fermion spectrum in the broken phase consists of a pair of split-up states which are, in general, mixtures of the original fermion and mirror fermion. For zero mixing the fermion masses are given by the renormalized vacuum expectation value of the scalar field times the renormalized Yukawa couplings. The possible large values of the renormalized Yukawa couplings open up the possibility of decoupling the mirror fermion by a very large mass (and zero mixing). In fact, if there is a non-trivial fixed point for Yukawa couplings as suggested by the qualitative behaviour of the two-loop β-functions, then the renormalized Yukawa coupling and the mass of the mirror fermion can be infinitely large. The decoupling of mirror fermions is only difficult if there is an upper limit for the renormalized Yukawa couplings. The advantage of the decoupling by a heavy mass is that it can be extended immediately to the case of weak gauge interactions, unlike the decoupling with zero coupling and zero mixing suggested in ref. [15]. Therefore in the numerical simulations one can try to make the mirror fermion heavy and its mixing to the light fermion small. This will be our approach in the present paper. Of course, it remains still interesting whether the other way of decoupling is possible or not, but up to now we did not try to follow the suggestion of ref. [15]. Heavy mirror fermions can be obtained by large values of the bare Yukawa coupling of mirror fermions (G_χ), and therefore an extension of the numerical simulations in the symmetric phase to $G_\chi \neq 0$ can supplement the studies in the broken phase. We performed a series of runs for $G_\psi, G_\chi \neq 0$ at infinite bare quartic coupling ($\lambda = \infty$) and found a qualitatively very similar behaviour as in ref. [11] at $G_\chi = 0$. (These results will be published elsewhere.)

Besides the very important question of doubler- and mirror-fermion decoupling there are also other important issues in the broken phase, such as the problem of cut-off dependent limits on the scalar and fermion masses. These have to do with the behaviour of the β-functions. If the only fixed point is the infrared stable one at zero couplings, then the continuum limit is trivial and there are cut-off dependent upper limits for the scalar and fermion masses. The property that in some region of the couplings the perturbative β-function of the quartic scalar coupling is negative implies that there is also a lower limit for the Higgs-boson mass which depends on the value of the fermion mass. In the literature this is called "vacuum stability bound" [16]. Both upper and lower limits depend crucially on the properties of the continuum limit. If there is a non-trivial fixed point, then the continuum limit is non-trivial, there are no cut-off dependent upper limits and also the discussion of the vacuum stability bound is quite different from the case of a trivial continuum limit. Therefore the most important question is the fixed-point structure of the β-functions. To investigate this it is better to return first to the

symmetric phase where the study of the renormalization is easier. Under the assumption of triviality (no non-trivial fixed point) the simulation data presented in this paper can give some hints about the upper bounds in the broken phase. From the investigation of the λ-dependence one can also draw conclusions concerning the vacuum stability lower bound on the Higgs mass.

In general, the evaluation of the numerical simulation data in the broken phase is more difficult than in the symmetric phase. First of all, there is the zero-mass Goldstone boson due to spontaneous symmetry breaking. This causes serious finite size effects culminating in the infrared singularity of some zero-momentum Green's functions. There are elaborate techniques to deal with this [17] but in a first exploratory study these would be too demanding. Therefore here we shall follow simple pragmatic ways to extract the physical quantities. A second difficulty in the broken phase is that the scalar and fermion masses cannot be tuned separately. If, for instance, zero mixing between fermion and mirror fermion is assumed and the Higgs-boson mass is tuned to some desired value then the fermion masses are already determined by the renormalized couplings. In some range of renormalized couplings the implied scalar-fermion mass ratio can be either very small or very large, which makes the control of finite-volume effects in the numerical simulations difficult. (Note that this is different from the symmetric phase, where both scalar and fermion masses can be tuned by the hopping parameters at any values of the couplings.) The consequence for the present paper is that sometimes we have to live with possibly large finite-volume effects. Nevertheless, some efforts will be taken to see the change of the results with the lattice size.

An important requirement for the euclidean lattice formulation is the Osterwalder–Schrader reflection positivity [18]. This axiom plays an important rôle in the reconstruction of the quantum field theory in Minkowski space from the corresponding euclidean quantum field theory, because it implies the existence of a self-adjoint hamiltonian with non-negative spectrum. The problem of reflection positivity of lattice Yukawa models received up to now little attention (for lattice gauge theories with fermions see, for instance, ref. [19] and references therein). In the present paper this question will be considered in our formulation with mirror pairs of fermion fields.

In the next section the lattice action will be defined and the problem of reflection positivity will be investigated. In sect. 3 the renormalized parameters will be considered and the definitions suitable for numerical simulations in the broken phase will be given. Sect. 4 is devoted to lattice perturbation theory in the broken phase. The results of the numerical simulations will be presented and discussed in sects. 5 and 6. Sect. 5 is concentrated around the question of the mirror symmetry breaking and the possibility of making both doublers and mirror fermions heavy. In sect. 6 the vacuum stability bound will be discussed. The last section contains a short summary and some concluding remarks.

2. The lattice action and reflection positivity

Throughout this paper the same notations will be used as in ref. [11]. For the reader's convenience first we repeat a few basic formulas. The lattice action with a general field normalization is

$$\begin{aligned} S \equiv S_\phi + S_{\psi\chi\phi} = \sum_x \Big\{ & \mu_\phi \phi_x^+ \phi_x + \lambda (\phi_x^+ \phi_x)^2 - \kappa \sum_\mu \phi_{x+\hat{\mu}}^+ \phi_x \\ & + \mu_{\psi\chi} \big[(\bar{\chi}_x \psi_x) + (\bar{\psi}_x \chi_x) \big] - \sum_\mu \big[K_\psi (\bar{\psi}_{x+\hat{\mu}} \gamma_\mu \psi_x) + K_\chi (\bar{\chi}_{x+\hat{\mu}} \gamma_\mu \chi_x) \big] \\ & + K_r \sum_\mu \big[(\bar{\chi}_x \psi_x) - (\bar{\chi}_{x+\hat{\mu}} \psi_x) + (\bar{\psi}_x \chi_x) - (\bar{\psi}_{x+\hat{\mu}} \chi_x) \big] \\ & + G_\psi (\bar{\psi}_x [\phi_{1x} - i\gamma_5 \phi_{2x}] \psi_x) + G_\chi (\bar{\chi}_x [\phi_{1x} + i\gamma_5 \phi_{2x}] \chi_x) \Big\} . \end{aligned} \tag{1}$$

Here x is a lattice point and the sum Σ_μ runs over eight directions of the neighbours, $\hat{\mu}$ is the unit vector in the direction of μ. The fields for the mirror fermion pair are ψ_x and χ_x, the complex scalar field is $\phi_x \equiv \phi_{1x} + i\phi_{2x}$. A normalization convenient for the numerical simulations is defined by

$$\mu_\phi = 1 - 2\lambda , \qquad K_\psi = K_\chi \equiv K , \qquad K_r \equiv rK , \qquad \bar{\mu} \equiv \mu_{\psi\chi} + 8rK = 1 . \tag{2}$$

The fermionic part of the action $S_{\psi\chi\phi}$ can be written with the help of the "fermion matrix" $Q(\phi)_{yx}$ as

$$S_{\psi\chi\phi} = \sum_{x,y} \bar{\Psi}_y Q(\phi)_{yx} \Psi_x . \tag{3}$$

Here the fermion field $\Psi_x \equiv (\psi_x, \chi_x)$ stands for the mirror pair, and the $8 \otimes 8$ matrix Q is given in the fermion–mirror-fermion basis in $4 \otimes 4$ block notation by

$$Q(\phi)_{yx} = \delta_{yx} \begin{pmatrix} G_\psi (\phi_{1x} - i\gamma_5 \phi_{2x}) & \bar{\mu} \\ \bar{\mu} & G_\chi (\phi_{1x} + i\gamma_5 \phi_{2x}) \end{pmatrix} - K \sum_\mu \delta_{y,x+\hat{\mu}} \begin{pmatrix} \gamma_\mu & r \\ r & \gamma_\mu \end{pmatrix} . \tag{4}$$

Here r is the Wilson parameter, which is usually chosen to be 1. For negative indices the definition of the euclidean Dirac-matrices is $\gamma_{-\mu} = -\gamma_\mu$.

In order to be able to use the Hybrid Monte Carlo algorithm for dynamical fermions in the numerical simulations, the fermion spectrum has to be flavour-

doubled. Therefore the fermionic part of the lattice action will be, instead of eq. (3),

$$S_{\psi\chi\phi} = \sum_{f=1,2} \sum_{x,y} \bar{\Psi}_y^{(f)} Q(\phi)_{yx}^{(f)} \Psi_x^{(f)}. \tag{5}$$

For the value $f=1$ of the flavour index the fermion matrix is given by eq. (4): $Q^{(1)} = Q$, but for the other value $f=2$ the adjoint is taken: $Q^{(2)} = Q^+$. This means that the ψ-field of the second flavour ($\psi^{(2)}$) is a mirror-field with respect to the ψ-field of the first one ($\psi^{(1)}$). The flavour doubling of the fermion fields leads also to an extension of the chiral symmetry from $U(1)_L \otimes U(1)_R$ to $U(1)_L \otimes U(1)_R \otimes U(1)_{1-2}$ [11]. If the model is described in terms of the left-handed fields (the right-handed fields are represented by the left-handed component of the charge-conjugate field as $\psi_{cL} \equiv C\bar{\psi}_R^T$), then the quantum numbers of the 8 fermion fields and of the Higgs field are

	$U(1)_L$	$U(1)_R$	$U(1)_{1-2}$		$U(1)_L$	$U(1)_R$	$U(1)_{1-2}$
$\psi_L^{(1)}$:	1	0	1	$\psi_L^{(2)}$:	0	1	−1
$\psi_{cL}^{(1)}$:	0	−1	−1	$\psi_{cL}^{(2)}$:	−1	0	1
$\chi_L^{(1)}$:	0	1	1	$\chi_L^{(2)}$:	1	0	−1
$\chi_{cL}^{(1)}$:	−1	0	−1	$\chi_{cL}^{(2)}$:	0	−1	1
ϕ:	1	−1	0				

(6)

The mass terms allowed by the chiral symmetry $U(1)_L \otimes U(1)_R \otimes U(1)_{1-2}$ are those connecting $\psi^{(1)}$ with $\chi^{(1)}$ or $\psi^{(2)}$ with $\chi^{(2)}$ but not $\psi^{(1)}$ with $\psi^{(2)}$ and $\chi^{(1)}$ with $\chi^{(2)}$ (these latter are forbidden by $U(1)_{1-2}$). The vacuum expectation value of the scalar field breaks $U(1)_L \otimes U(1)_R$ to its diagonal subgroup, but $U(1)_{1-2}$ is not spontaneously broken, at least in the phase which is considered in this article. A "chiral" set of fields can be defined by the requirement that no mass term is allowed by the symmetry and/or generated by spontaneous symmetry breaking. In this sense, for instance, the subset $\{\psi_L^{(1)}, \psi_{cL}^{(1)}\}$ is "chiral" and "anomalous" (that is, has a non-zero U(1)-anomaly). A subset like $\{\psi_L^{(1)}, \psi_{cL}^{(1)}, \chi_L^{(1)}, \chi_{cL}^{(1)}\}$ is "non-chiral" and "non-anomalous". Finally, the subset $\{\psi_L^{(1)}, \psi_{cL}^{(1)}, \psi_L^{(2)}, \psi_{cL}^{(2)}\}$, which is obtained after decoupling the mirror (χ-) fields, is "chiral" and "non-anomalous". (With respect to the subgroup $U(1)_L \otimes U(1)_R$ this latter subset is "non-chiral", but there is no reason why only this subgroup should be considered.) Therefore, in some general sense the subset $\{\psi_L^{(1)}, \psi_{cL}^{(1)}, \psi_L^{(2)}, \psi_{cL}^{(2)}\}$ is similar to a fermion family in the standard model, although there the pattern of anomaly cancellation is different.

The above form of the action is convenient for the physical interpretation of the fermion spectrum in the broken phase, but for some purposes, like the hopping parameter expansion in the symmetric phase or the proof of reflection positivity, it

is better to introduce another form based on the fields

$$\psi_{Ax} \equiv \psi_{Lx} + \chi_{Rx}, \qquad \psi_{Bx} \equiv \chi_{Lx} + \psi_{Rx}, \qquad \bar{\psi}_{Ax} \equiv \bar{\psi}_{Lx} + \bar{\chi}_{Rx}, \qquad \bar{\psi}_{Bx} \equiv \bar{\chi}_{Lx} + \bar{\psi}_{Rx}. \tag{7}$$

Denoting now the (ψ_A, ψ_B)-pair by $\Psi_x \equiv (\psi_{Ax}, \psi_{Bx})$, and using the field normalization condition in eq. (2), $\bar{\mu} = 1$, the fermion matrix in eq. (3) becomes

$$\bar{Q}(\phi)_{yx} = \begin{pmatrix} \delta_{yx} - K\Sigma_\mu \delta_{y,x+\hat{\mu}}(\gamma_\mu + r) & \delta_{yx}\phi_x(G_\alpha - \gamma_5 G_\beta) \\ \delta_{yx}\phi_x^+(G_\alpha + \gamma_5 G_\beta) & \delta_{yx} - K\Sigma_\mu \delta_{y,x+\hat{\mu}}(\gamma_\mu + r) \end{pmatrix}. \tag{8}$$

The coupling constant combinations G_α, G_β are defined as

$$G_\alpha \equiv \tfrac{1}{2}(G_\psi + G_\chi), \qquad G_\beta \equiv \tfrac{1}{2}(G_\psi - G_\chi). \tag{9}$$

In the rest of this section the reflection positivity of chiral Yukawa models will be investigated in the lattice formulation with mirror pairs of fermion fields. The $U(1)_L \otimes U(1)_R$ symmetric model will explicitly be considered, but the results can immediately be generalized to other cases, as for instance to the $SU(2)_L \otimes SU(2)_R$ symmetric model. The positivity axiom asserts that there exists an antilinear operator Θ which transforms an arbitrary function F of the fields at positive times into a function ΘF of fields at negative times such that

$$\langle (\Theta F) F \rangle \geqslant 0. \tag{10}$$

The time reflection of the points can be defined on the lattice in two different ways: one can reflect either with respect to a plane between two time layers, say $t = 0$ and $t = 1$, which we call link-reflection, or with respect to the $t = 0$ plane, which is called site-reflection. The transformation in the first case is $t \to 1 - t$, in the second case $t \to -t$. If reflection positivity holds for either type of reflections a bounded positive transfer matrix can be defined for time shifts with an even distance [19, 20]. Since the definition of the transfer matrices depends on Θ, they can be different, and also the regions of bare parameter space where they are positive can, in principle, be different. Of course, in the continuum limit when the lattice spacing is going to zero, the positivity of any of them is sufficient to guarantee the existence of a self-adjoint hamiltonian with non-negative spectrum. At finite lattice spacings, for instance, in numerical simulations, the best thing is to have reflection positivity of both kinds, because then for the determination of the spectrum one can safely consider correlations at arbitrary time distances and the positive transfer matrix is the usual one, which acts on wave functions defined at fixed times, e.g. $t = 0$ [21].

Let us first consider the link-reflection positivity condition, that is the time reflection $t \to 1-t$. In this case the effect of the antilinear operator Θ on the fields in the $U(1)_L \otimes U(1)_R$ symmetric Yukawa model is (with $x = \{x, t\}$):

$$\Theta\phi_{x,t} = \phi^+_{x,1-t}, \qquad \Theta\Psi_{x,t} = \overline{\Psi}_{x,1-t}\gamma_4, \qquad \Theta\overline{\Psi}_{x,t} = \gamma_4\Psi_{x,1-t}. \tag{11}$$

The piece of the action connecting the two time-halfs of the space can therefore be written as

$$S_0 = -2\kappa\sum_x \phi_{x,1}(\Theta\phi_{x,1})$$

$$-K\sum_{l=A,B}\sum_x \{\Psi_{lx,1}(1-r\gamma_4)(\Theta\Psi_{lx,1}) + \overline{\Psi}_{lx,1}(1+r\gamma_4)(\Theta\overline{\Psi}_{lx,1})\}. \tag{12}$$

Here the form of the lattice action in eq. (8) was used for convenience. Since S_0 does not depend on the local Yukawa interactions, reflection positivity can be proven for $\kappa \geqslant 0$ in the same way as for the pure scalar model and for free fermions [20]. In case of non-zero Yukawa couplings the non-negativity of the scalar hopping parameter κ seems to be crucial. In principle, for $\kappa < 0$ one can try to introduce a different Θ-mapping, but for non-zero Yukawa coupling we did not succeed to find a suitable choice. (The fermion hopping parameter K can be negative, but negative K can be transformed away to a positive one by going to the opposite corners of the Brillouin zone [11].)

In case of the site-reflection positivity condition the Θ-mapping is defined in the same way as in eq. (11), only $1-t$ is replaced everywhere by $-t$. The proof of reflection positivity for $r = 1$ goes along the same lines as in ref. [19]. Defining the $t = 0$ field variables by

$$\phi_x \equiv \phi_{x,0}, \qquad \xi_x \equiv \tfrac{1}{2}(1+\gamma_4)\Psi_{x,0}, \qquad \xi^+_x \equiv \overline{\Psi}_{x,0}\tfrac{1}{2}(1+\gamma_4),$$

$$\eta^{\mathrm{T}}_x \equiv -\overline{\Psi}_{x,0}\tfrac{1}{2}(1-\gamma_4), \qquad \eta^{+\mathrm{T}}_x \equiv \tfrac{1}{2}(1-\gamma_4)\Psi_{x,0}, \tag{13}$$

the interactive part of the $t = 0$ piece of the action on the A, B-basis is

$$S_{0,\mathrm{int}} = \sum_x \{G_\alpha\phi^+_x(\xi^+_{\mathrm{B}x}\xi_{\mathrm{A}x} + \eta^+_{\mathrm{A}x}\eta_{\mathrm{B}x}) + G_\alpha\phi_x(\xi^+_{\mathrm{A}x}\xi_{\mathrm{B}x} + \eta^+_{\mathrm{B}x}\eta_{\mathrm{A}x})$$

$$+G_\beta\phi^+_x(\eta^{\mathrm{T}}_{\mathrm{B}x}\xi_{\mathrm{A}x} - \xi^+_{\mathrm{B}x}\eta^{+\mathrm{T}}_{\mathrm{A}x}) + G_\beta\phi_x(-\eta^{\mathrm{T}}_{\mathrm{A}x}\xi_{\mathrm{B}x} + \xi^+_{\mathrm{A}x}\eta^{+\mathrm{T}}_{\mathrm{B}x})\}. \tag{14}$$

The total $t = 0$ action can be written in matrix notation as

$$S_0 \equiv (\xi^+ B_\xi \xi) + (\eta^+ B_\eta \eta) + (\eta^{\mathrm{T}} C \xi) + (\xi^+ C^+ \eta^{+\mathrm{T}}). \tag{15}$$

The matrices $B_{\xi,\eta}$ and C occurring in the proof of reflection positivity [19] are, in a block notation on the A, B-basis

$$B_\xi = \begin{pmatrix} B_0 & G_\alpha \phi_x \\ G_\alpha \phi_x^+ & B_0 \end{pmatrix}, \quad B_\eta = \begin{pmatrix} B_0 & G_\alpha \phi_x^+ \\ G_\alpha \phi_x & B_0 \end{pmatrix},$$

$$C = \begin{pmatrix} C_0 & -G_\beta \phi_x \\ G_\beta \phi_x^+ & C_0 \end{pmatrix}. \tag{16}$$

Here B_0 and C_0 are the hermitian matrices occurring in the case of free Wilson fermions.

A sufficient condition for reflection positivity is the positivity of the matrices $B_{\xi,\eta}$, which is satisfied for $\lambda = \infty$ and

$$|K| < \tfrac{1}{6}(1 - |G_\alpha|) \tag{17}$$

irrespective of the value of the other bare parameters. It is remarkable that the γ_5 piece of the Yukawa coupling proportional to G_β does not influence the positivity domain at all. Correspondingly, in case of simple Yukawa models with one component scalar fields, Wilson fermions and local Yukawa couplings, the pseudoscalar couplings do not squeeze the positivity domain, unlike the scalar ones, for which a bound similar to eq. (17) holds. Obviously, the bound in eq. (17) cannot be satisfied for large bare scalar Yukawa couplings. In some special cases one can, however, derive site-reflection positivity also for very large bare Yukawa couplings by starting from another form of the action with composite fermion fields (similar to the ψ_x' field in ref. [9]). Without going into details here we just remark that, for instance, at $\lambda = \infty$ and $G_\beta = 0$ a sufficient condition in terms of $K_\infty \equiv K/G_\alpha$ is

$$|K_\infty| < \tfrac{1}{6}\left(1 - |G_\alpha|^{-1}\right). \tag{18}$$

This is interesting for small G_α^{-1} (that is for large G_α), where the relevant fermion hopping parameter is K_∞.

It is remarkable that, although the parameter region where link-reflection positivity could be proven is much wider than the one for site-reflection positivity, there is a region at negative κ and $\lambda = \infty$ where the site-reflection positivity condition could be proven but the link-reflection positivity condition not. As it was remarked before, this is not a contradiction, but one has also to keep in mind that the above proofs give only sufficient conditions and not necessary ones. Therefore, the full domain of reflection positivity can, in fact, be larger.

3. Renormalized parameters

The difficulty for the numerical simulations in the broken phase is the infrared singularity of some Green's functions at zero four-momentum, due to the presence of massless Goldstone bosons. The finite volume acts as an infrared regulator. Therefore there are very large finite-volume effects even in large volumes. In case of the O(N)-symmetric pure scalar models there is by now an impressive amount of ingenious work done, which shows that the problem can, in fact, be solved in a theoretically clean and rather appealing way (see, for instance refs. [17] and [22]). In practice, however, the procedure is rather demanding because it requires the introduction of an external source and the careful study of finite-size effects on large lattices. Another way to deal with the problem is to introduce the gauge interaction which has to be considered at some point anyway and which renders the Goldstone bosons massive [23]. The difficulty in this case is that one has to deal with a relatively large ratio of the Higgs-boson mass to W-boson mass, which is about 8–10 at the upper limit [24,25]. In a first exploratory study both these ways of dealing with the Goldstone boson problem would be too difficult. Therefore one has to return to simple pragmatic ways which are known to give satisfactory results in pure scalar ϕ^4 models [26,27].

For the definition of the vacuum expectation value of the scalar field on a finite lattice one has to take into account the drift of the direction of the symmetry breaking. For a given configuration of the scalar field the average of the field over the $L^3 \cdot T$ lattice is

$$\phi \equiv \frac{1}{L^3 T} \sum_x \phi_x \,. \tag{19}$$

An infinitesimal external source field is imagined to point in the direction of ϕ, given in our case by the phase angle α:

$$\phi = |\phi| \mathrm{e}^{i\alpha} \,. \tag{20}$$

The vacuum expectation value is then defined by the absolute value of the average field:

$$v \equiv \langle |\phi| \rangle \,. \tag{21}$$

In order to have the imagined external source field always in the direction of the real axis, a global $\mathrm{U(1)_L} \otimes \mathrm{U(1)_R}$ transformation is applied to the field configuration. This defines the longitudinal ($\phi_{\mathrm{L}x}$) and transverse ($\phi_{\mathrm{T}x}$) field components:

$$\phi'_x = \mathrm{e}^{-i\alpha} \phi_x \equiv \phi_{\mathrm{L}x} + i\phi_{\mathrm{T}x} \,. \tag{22}$$

Similarly, since $\alpha = \alpha_L - \alpha_R$ [11], for the chiral components of the fermion fields we have:

$$\psi'_{Lx} = e^{-i\alpha}\psi_{Lx}, \quad \psi'_{Rx} = \psi_{Rx}, \quad \bar{\psi}'_{Lx} = \bar{\psi}_{Lx}e^{i\alpha}, \quad \bar{\psi}'_{Rx} = \bar{\psi}_{Rx},$$

$$\chi'_{Rx} = e^{-i\alpha}\chi_{Rx}, \quad \chi'_{Lx} = \chi_{Lx}, \quad \bar{\chi}'_{Rx} = \bar{\chi}_{Rx}e^{i\alpha}, \quad \bar{\chi}'_{Lx} = \bar{\chi}_{Lx}. \tag{23}$$

(This holds for the $f = 1$ flavour, for $f = 2$ the transformations of ψ and χ are exchanged.)

In a numerical simulation the renormalized quantities for the scalar field are defined by the timeslices of the longitudinal and transverse correlations

$$S_{Lt} \equiv \frac{1}{L^3}\sum_x \langle \phi_{Lxt}\phi_{L00}\rangle_c = \frac{1}{L^3}\sum_x \left(\langle \phi_{Lxt}\phi_{L00}\rangle - v^2\right),$$

$$S_{Tt} \equiv \frac{1}{L^3}\sum_x \langle \phi_{Txt}\phi_{T00}\rangle. \tag{24}$$

Here it was taken into account that $\langle \phi_{Lx}\rangle = v$ and $\langle \phi_{Tx}\rangle = 0$. The behaviour of the longitudinal correlations is dominated by the physical Higgs boson mass m_L. On a periodic lattice with time extension T one can determine m_L, at sufficiently large time separation t, from a fit

$$S_{Lt} = a + b(e^{-m_L t} + e^{-m_L(T-t)}). \tag{25}$$

The constant a is due to the non-zero expectation value of ϕ_{Lx} [28].

The wave-function renormalization constants of the scalar field have an infrared singularity at zero four-momentum, but they can be extracted from the behaviour at non-zero momenta [26, 27]. In case of a not very large lattice the lowest non-zero momentum can be used and then suitable definitions of Z_L and Z_T are

$$Z_L \equiv \left(m_L^2 + 4\sin^2\frac{\pi}{T}\right)\sum_{x=(xt)} \cos\left(\frac{2\pi}{T}t\right)\langle \phi_{Lx}\phi_{L0}\rangle_c,$$

$$Z_T = 4\sin^2\frac{\pi}{T}\sum_{x=(xt)} \cos\left(\frac{2\pi}{T}t\right)\langle \phi_{Tx}\phi_{T0}\rangle. \tag{26}$$

The renormalized vacuum expectation value v_R and renormalized quartic scalar coupling g_R are then defined as

$$v_R = \frac{v}{\sqrt{Z_T}} = \frac{\langle \phi_{Lx}\rangle}{\sqrt{Z_T}}, \qquad g_R = \frac{3m_L^2}{v_R^2}. \tag{27}$$

The renormalized quantities in the fermionic sector are defined by the 2-point function of the transformed fermion field $\Psi' = (\psi'\chi')$:

$$\tilde{\Delta}_\Psi(p) \equiv \sum_x e^{-ip\cdot(y-x)} \langle \Psi'_y \bar{\Psi}'_x \rangle . \tag{28}$$

For small momenta let the behaviour of $\tilde{\Delta}_\Psi$ and $\tilde{\Delta}_\Psi^{-1}$ be

$$\tilde{\Delta}_\Psi \simeq A - ip\cdot\gamma B, \qquad \tilde{\Delta}_\Psi^{-1} \simeq M + ip\cdot\gamma N. \tag{29}$$

For the fermion fields we use antiperiodic boundary conditions in the time direction such that the smallest momenta in the time direction are $\pm\pi/T$. Therefore suitable definitions of A and B are

$$\begin{aligned} A &= \frac{1}{2}\left[\tilde{\Delta}_\Psi\left(0,0,0,+\frac{\pi}{T}\right) + \tilde{\Delta}_\Psi\left(0,0,0,-\frac{\pi}{T}\right)\right] \\ &= \sum_{x=\{xt\}} \cos\left[\frac{\pi}{T}t\right] \langle \Psi'_0 \bar{\Psi}'_x \rangle \equiv \begin{pmatrix} a_1 & a \\ a & a_2 \end{pmatrix}, \\ \gamma_4 B &= \frac{i}{2\sin(\pi/T)}\left[\tilde{\Delta}_\Psi\left(0,0,0,+\frac{\pi}{T}\right) - \tilde{\Delta}_\Psi\left(0,0,0,-\frac{\pi}{T}\right)\right] \\ &= -\sum_{x=\{xt\}} \frac{\sin[\pi t/T]}{\sin(\pi/T)} \langle \Psi'_0 \bar{\Psi}'_x \rangle \equiv \gamma_4 \begin{pmatrix} b_1 & b \\ b & b_2 \end{pmatrix}. \end{aligned} \tag{30}$$

Here the matrices are in a block notation in the (ψ', χ') space. The connection to the matrices M, N in the inverse propagator is

$$M \equiv \begin{pmatrix} m_1 & m \\ m & m_2 \end{pmatrix} = A^{-1} = (a^2 - a_1 a_2)^{-1} \begin{pmatrix} -a_2 & a \\ a & -a_1 \end{pmatrix},$$

$$N \equiv \begin{pmatrix} n_1 & n \\ n & n_2 \end{pmatrix} = A^{-1} B A^{-1}$$

$$= (a^2 - a_1 a_2)^{-1} \begin{pmatrix} a^2 b_2 + a_2^2 b_1 - 2a a_2 b & a^2 b - a a_1 b_2 - a a_2 b_1 + a_1 a_2 b \\ a^2 b - a a_1 b_2 - a a_2 b_1 + a_1 a_2 b & a^2 b_1 + a_1^2 b_2 - 2a a_1 b \end{pmatrix}. \tag{31}$$

The wave-function renormalization has to transform N to the unit matrix:

$$Z_\psi^{1/2\mathrm{T}} N Z_\psi^{1/2} = \begin{pmatrix} 1 & 0 \\ 0 & 1 \end{pmatrix}. \tag{32}$$

In the symmetric phase $Z_\Psi^{1/2}$ is diagonal, but now, due to $n \neq 0$, a rotation is also needed:

$$Z_\Psi^{1/2} = \begin{pmatrix} \cos\zeta & -\sin\zeta \\ \sin\zeta & \cos\zeta \end{pmatrix} \begin{pmatrix} \sqrt{Z_\psi} & 0 \\ 0 & \sqrt{Z_\chi} \end{pmatrix}. \tag{33}$$

In terms of the matrix elements of N in eq. (31) we have

$$\zeta = \tfrac{1}{2}\arcsin \frac{\operatorname{sgn}(n_1 - n_2)\cdot 2n}{\sqrt{(n_1 - n_2)^2 + 4n^2}},$$

$$Z_\psi = 2\left[n_1 + n_2 + \operatorname{sgn}(n_1 - n_2)\sqrt{(n_1 - n_2)^2 + 4n^2}\right]^{-1},$$

$$Z_\chi = 2\left[n_1 + n_2 - \operatorname{sgn}(n_1 - n_2)\sqrt{(n_1 - n_2)^2 + 4n^2}\right]^{-1}. \tag{34}$$

Multiplying the unrenormalized mass matrix M by $Z_\Psi^{1/2}$ from left and right gives the renormalized mass matrix M_R:

$$M_R \equiv Z_\Psi^{1/2T} M Z_\Psi^{1/2} \equiv \begin{pmatrix} G_{R\psi} v_R & \mu_R \\ \mu_R & G_{R\chi} v_R \end{pmatrix}. \tag{35}$$

This defines the renormalized off-diagonal mass μ_R and the renormalized Yukawa couplings $G_{R\psi}$ and $G_{R\chi}$ (the renormalized vacuum expectation value v_R is given by eq. (27)). In terms of the matrix elements of M in eq. (31) we have

$$\mu_R = \sqrt{Z_\psi Z_\chi}\left[m\cos(2\zeta) - \tfrac{1}{2}(m_1 - m_2)\sin(2\zeta)\right],$$

$$G_{R\psi} = \frac{Z_\psi}{v_R}\left[\tfrac{1}{2}(m_1 + m_2) + \tfrac{1}{2}(m_1 - m_2)\cos(2\zeta) + m\sin(2\zeta)\right],$$

$$G_{R\chi} = \frac{Z_\chi}{v_R}\left[\tfrac{1}{2}(m_1 + m_2) - \tfrac{1}{2}(m_1 - m_2)\cos(2\zeta) - m\sin(2\zeta)\right]. \tag{36}$$

The renormalized fermion mass matrix (35) can be diagonalized by a rotation with an angle α_R. Let the mass eigenvalues be denoted by μ_{1R} and μ_{2R}. The corresponding eigenstates are then mixtures of the original ψ- and χ-states with the

mixing angle α_R. The explicit relations to the matrix elements of M_R are

$$\sin\alpha_R = \frac{\mu_R\sqrt{2}}{\sqrt{v_R^2(G_{R\psi}-G_{R\chi})^2+4\mu_R^2}+v_R|G_{R\psi}-G_{R\chi}|\sqrt{v_R^2(G_{R\psi}-G_{R\chi})^2+4\mu_R^2}},$$

$$\mu_{1R} = \tfrac{1}{2}\Big[v_R(G_{R\psi}+G_{R\chi}) + \mathrm{sgn}(G_{R\psi}-G_{R\chi})\sqrt{v_R^2(G_{R\psi}-G_{R\chi})^2+4\mu_R^2}\Big],$$

$$\mu_{2R} = \tfrac{1}{2}\Big[v_R(G_{R\psi}+G_{R\chi}) - \mathrm{sgn}(G_{R\psi}-G_{R\chi})\sqrt{v_R^2(G_{R\psi}-G_{R\chi})^2+4\mu_R^2}\Big]. \tag{37}$$

These expressions are valid at the zero corner of the Brillouin zone. The other corners at $p=(e_1\pi, e_2\pi, e_3\pi, e_4\pi)$; $e_{1,2,3,4}=0,1$ can be reached by a transformation of the fermion field

$$\Psi_x \to (-1)^{e_1x_1+e_2x_2+e_3x_3+e_4x_4}\Psi_x, \qquad \bar{\Psi}_x \to (-1)^{e_1x_1+e_2x_2+e_3x_3+e_4x_4}\bar{\Psi}_x. \tag{38}$$

If one wants to calculate the fermionic renormalized quantities at the other corners, then one has to take these transformed fields in eq. (30). Otherwise the same formulae as in eqs. (31)–(37) apply.

4. Perturbation theory on the lattice

Green's functions and other quantities in the Yukawa model can be studied by means of perturbation theory. In bare perturbation theory the expansions are in powers of the bare couplings, namely the scalar self-coupling λ and the Yukawa couplings G_ψ and G_χ. Reexpressing these in terms of the corresponding renormalized couplings leads to renormalized perturbation theory. In order to obtain Feynman rules similar to the case of perturbation theory in the continuum, the fields and couplings have to be rescaled. We define the bare scalar field ϕ_0 and its components ϕ_{0k} through

$$\sqrt{\kappa}\,\phi = \phi_0 = \frac{1}{\sqrt{2}}(\phi_{01}+i\phi_{02}). \tag{39}$$

The lattice lagrangean for the scalar field is then

$$\mathscr{L}_\phi = (\partial_\mu\phi_0)^+\partial^\mu\phi_0 - \frac{m_0^2}{2}\phi_0^+\phi_0 + \frac{g_0}{6}(\phi_0^+\phi_0)^2, \tag{40}$$

where ∂_μ denotes a lattice derivative (i.e. finite difference) and the bare mass m_0 and bare coupling g_0 are given by

$$m_0^2 = 16 - \frac{2\mu_\phi}{\kappa}, \qquad g_0 = \frac{6\lambda}{\kappa^2}. \tag{41}$$

The potential has its minima at

$$\sqrt{2}|\phi_0(x)| = s_0 = \sqrt{3m_0^2/g_0} \tag{42}$$

and the shifted fields are defined by

$$\sigma(x) = \varphi_{01}(x) = \phi_{01}(x) - s_0, \qquad \pi(x) = \varphi_{02}(x) = \phi_{02}(x). \tag{43}$$

In terms of these fields the lagrangian is

$$\mathscr{L}_\phi = \tfrac{1}{2}(\partial_\mu\sigma)^2 + \frac{m_0^2}{2}\sigma^2 + \tfrac{1}{2}(\partial_\mu\pi)^2 + \frac{1}{3!}\sqrt{3g_0}\,m_0\sigma(\sigma^2+\pi^2)$$
$$+ \frac{g_0}{4!}(\sigma^2+\pi^2)^2 + \text{const.} \tag{44}$$

From this expression we read off the Feynman rules for the scalar field. The perturbative expansions are most conveniently derived in momentum space. On a finite $L^3 \cdot T$ lattice the allowed momenta are in the Brillouin zone

$$p_i = \frac{2\pi}{L} n_i, \qquad n_i = 0,1,2,\ldots,L-1, \quad i = 1,2,3$$
$$p_4 = \frac{2\pi}{T}(n_4 + \delta_4), \qquad n_4 = 0,1,2,\ldots,T-1, \tag{45}$$

where for bosons $\delta_4 = 0$ and for fermions $\delta_4 = \frac{1}{2}$. For later convenience we introduce the following abbreviations:

$$\hat{p}_\mu = 2\sin\left(\tfrac{1}{2}p_\mu\right), \qquad \bar{p}_\mu = \sin(p_\mu). \tag{46}$$

The scalar propagator is diagonal in the field components with

$$\tilde{\Delta}_{11}(p) = \left(\hat{p}^2 + m_0^2\right)^{-1}, \qquad \tilde{\Delta}_{22}(p) = \left(\hat{p}^2\right)^{-1} \quad (p \neq 0). \tag{47}$$

The scalar three-point vertices are

$$-g_0 s_0, \qquad \text{for } \sigma\sigma\sigma, \tag{48}$$

$$-\tfrac{1}{3} g_0 s_0, \qquad \text{for } \pi\pi\sigma, \tag{49}$$

and the scalar four-point vertex is

$$-g_0 S_{ijkl}, \qquad i,j,k,l = 1,2 \tag{50}$$

with

$$S_{ijkl} = \tfrac{1}{3}(\delta_{ij}\delta_{kl} + \delta_{ik}\delta_{jl} + \delta_{il}\delta_{jk}). \tag{51}$$

The bare fermion and mirror fermion fields are defined by

$$\psi_0 = \sqrt{2K}\,\psi, \qquad \chi_0 = \sqrt{2K}\,\chi \tag{52}$$

and the free part of the fermion lagrangian for one flavour is

$$\mathcal{L}_\psi = -\sum_{\mu=1}^{4} \left\{ \tfrac{1}{2}(\bar{\psi}_{0,x+\hat{\mu}} - \bar{\psi}_{0,x-\hat{\mu}})\gamma_\mu \psi_{0,x} + \tfrac{1}{2} r(\bar{\chi}_{0,x+\hat{\mu}} + \bar{\chi}_{0,x-\hat{\mu}} - 2\bar{\chi}_{0,x})\psi_{0,x} + (\psi \leftrightarrow \chi) \right\}$$

$$+ \mu_0(\bar{\chi}_{0,x}\psi_{0,x} + \bar{\psi}_{0,x}\chi_{0,x}) + G_{0\psi} s_0 \bar{\psi}_{0,x}\psi_{0,x} + G_{0\chi} s_0 \bar{\chi}_{0,x}\chi_{0,x} \tag{53}$$

with

$$\mu_0 = \frac{\mu_{\psi\chi}}{2K}, \qquad G_{0\psi} = \frac{G_\psi}{2K\sqrt{2\kappa}}, \qquad G_{0\chi} = \frac{G_\chi}{2K\sqrt{2\kappa}}. \tag{54}$$

The explicit mass terms are due to the spontaneous breakdown of symmetry. For simplicity of the notation we display the conventions for one fermion flavour only. The perturbative results below, however, refer to the full model with two flavours of fermions and mirror fermions. In terms of the two-component vector

$$\Psi_0 = \begin{pmatrix} \psi_0 \\ \chi_0 \end{pmatrix} \tag{55}$$

the free fermion action can be written as

$$S_\psi = \sum_{xy} \bar{\Psi}_{0,y} W_{yx} \Psi_{0,x}. \tag{56}$$

W_{yx} is a two-by-two matrix in (ψ, χ)-space whose Fourier transform is

$$\tilde{W}(p) = \sum_x e^{-ip\cdot(y-x)} W_{yx} = \begin{pmatrix} i\gamma\cdot\bar{p} + \mu_{0\psi} & \mu_p \\ \mu_p & i\gamma\cdot\bar{p} + \mu_{0\chi} \end{pmatrix}, \tag{57}$$

where

$$\mu_p = \mu_0 + \frac{r}{2}\hat{p}^2, \qquad \mu_{0\psi} = G_{0\psi} s_0, \qquad \mu_{0\chi} = G_{0\chi} s_0. \tag{58}$$

The fermion propagator is given by

$$\tilde{W}(p)^{-1} = \tilde{D}(p)^{-1} \begin{pmatrix} (\bar{p}^2 + \mu_{0\chi}^2)\mu_{0\psi} - \mu_p^2\mu_{0\chi} & (\bar{p}^2 + \mu_p^2 - \mu_{0\psi}\mu_{0\chi})\mu_p \\ (\bar{p}^2 + \mu_p^2 - \mu_{0\psi}\mu_{0\chi})\mu_p & (\bar{p}^2 + \mu_{0\psi}^2)\mu_{0\chi} - \mu_p^2\mu_{0\psi} \end{pmatrix}$$

$$- i\gamma\cdot\bar{p}\tilde{D}(p)^{-1} \begin{pmatrix} \bar{p}^2 + \mu_p^2 + \mu_{0\chi}^2 & -(\mu_{0\psi} + \mu_{0\chi})\mu_p \\ -(\mu_{0\psi} + \mu_{0\chi})\mu_p & \bar{p}^2 + \mu_p^2 + \mu_{0\psi}^2 \end{pmatrix}, \tag{59}$$

with

$$\tilde{D}(p) = (\bar{p}^2 + \mu_p^2 - \mu_{0\psi}\mu_{0\chi})^2 + \bar{p}^2(\mu_{0\psi} + \mu_{0\chi})^2. \tag{60}$$

The Yukawa interaction is

$$S_Y = \sum_x \bar{\Psi}_{0,x} V_i \varphi_{0i} \Psi_{0,x}, \tag{61}$$

where the coupling matrices V_i are

$$V_i = \begin{pmatrix} G_{0\psi}\Gamma_i & 0 \\ 0 & G_{0\chi}\Gamma_i^+ \end{pmatrix} \tag{62}$$

with

$$\Gamma_1 = 1, \qquad \Gamma_2 = -i\gamma_5. \tag{63}$$

The Yukawa interaction vertex between two fermions and the scalar field φ_{0i} is given by the matrix $-V_i$.

Given these Feynman rules the Green's functions and vertex functions can be calculated perturbatively in the usual way. Let us consider vertex functions

$$\Gamma^{(n_B, 2n_F)}(p_a), \qquad a = 1, \ldots, n_B + 2n_F$$

for n_B bosons, n_F fermions and n_F anti-fermions. They refer to the fields

$\phi, \psi, \chi, \bar{\psi}$ and $\bar{\chi}$ in the original normalization. Below we present results in the one-loop approximation. Momentum sums or integrals respectively only run over the Brillouin zone specified above. They are denoted by

$$\int_p = \frac{1}{L^3 T} \sum_p = (2\pi)^{-4} \int_0^{2\pi} \mathrm{d}^4 p \quad \text{if} \quad L, T = \infty. \tag{64}$$

If the integrand contains massless propagators the momentum sum is understood without the point $p = 0$.

$\Gamma^{(2,0)}$ is the negative inverse propagator of the field $\phi(x)$. It is diagonal in the field indices:

$$\Gamma^{(2,0)}(p) = \begin{pmatrix} \Gamma_\sigma(p) & 0 \\ 0 & \Gamma_\pi(p) \end{pmatrix}. \tag{65}$$

For the inverse π-propagator we find

$$\begin{aligned} -\frac{1}{2\kappa}\Gamma_\pi(p) = {} & \hat{p}^2 - \frac{g_0}{3}\int_q (\hat{q}^2 + m_0^2)^{-1} + \frac{g_0}{3}\int_q (\hat{q}^2)^{-1} - \frac{g_0}{3} m_0^2 \int_q (\hat{q}^2 + m_0^2)^{-1} \Big[\widehat{(p+q)^2}\Big]^{-1} \\ & + 8\int_q \tilde{D}(q)^{-1} \big\{ \bar{q}^2 \big(G_{0\psi}^2 + G_{0\chi}^2\big) - 2\mu_q^2 G_{0\psi} G_{0\chi} + 2 G_{0\psi}^2 G_{0\chi}^2 s_0^2 \big\} \\ & - 8\int_q \tilde{D}(q)^{-1} \tilde{D}(p+q)^{-1} \Big\{ \big(\bar{q}^2 G_{0\psi}^2 + G_{0\psi}^2 G_{0\chi}^2 s_0^2 - \mu_q^2 G_{0\psi} G_{0\chi} \big) \\ & \times \Big(\big(\overline{p+q}\big)^2 G_{0\psi}^2 + G_{0\psi}^2 G_{0\chi}^2 s_0^2 - \mu_{p+q}^2 G_{0\psi} G_{0\chi} \Big) s_0^2 \\ & - \big(\bar{q}^2 + \mu_q^2 - G_{0\psi} G_{0\chi} s_0^2 \big) \Big(\big(\overline{p+q}\big)^2 + \mu_{p+q}^2 - G_{0\psi} G_{0\chi} s_0^2 \Big) G_{0\psi} G_{0\chi} \mu_q \mu_{p+q} \\ & + \big(\bar{q}^2 + \mu_q^2 + G_{0\chi}^2 s_0^2 \big) \Big(\big(\overline{p+q}\big)^2 + \mu_{p+q}^2 + G_{0\chi}^2 s_0^2 \Big) G_{0\psi}^2 \bar{q} \cdot \overline{p+q} \\ & - \mu_q \mu_{p+q} \big(G_{0\psi} + G_{0\chi}\big)^2 G_{0\psi} G_{0\chi} s_0^2 \bar{q} \cdot \overline{p+q} + (\psi \leftrightarrow \chi) \Big\}. \end{aligned} \tag{66}$$

The π-field is massless and the inverse propagator behaves like

$$-\Gamma_\pi(p) = Z_\pi^{-1} \{ p^2 + \mathrm{O}(p^4) \}, \tag{67}$$

which defines the wave-function renormalization constant Z_π corresponding to Z_T in the infinite-volume limit.

Our result for the inverse σ-propagator is

$$
\begin{aligned}
-\frac{1}{2\kappa}\Gamma_\sigma(p) = {} & \hat{p}^2 + m_0^2 - g_0 \int_q \left(\hat{q}^2 + m_0^2\right)^{-1} \\
& - \frac{g_0}{3}\int_q (\hat{q}^2)^{-1} - \frac{3g_0}{2} m_0^2 \int_q \left(\hat{q}^2 + m_0^2\right)^{-1} \left[\widehat{(p+q)}^2 + m_0^2\right]^{-1} \\
& - \frac{g_0}{6} m_0^2 \int_q (\hat{q}^2)^{-1} \left[\widehat{(p+q)}^2\right]^{-1} + 24 \int_q \tilde{D}(q)^{-1} \\
& \times \left\{\bar{q}^2\left(G_{0\psi}^2 + G_{0\chi}^2\right) - 2\mu_q^2 G_{0\psi} G_{0\chi} + 2G_{0\psi}^2 G_{0\chi}^2 s_0^2\right\} \\
& + 8 \int_q \tilde{D}(q)^{-1} \tilde{D}(p+q)^{-1} \Big\{ \left(\bar{q}^2 G_{0\psi}^2 + G_{0\psi}^2 G_{0\chi}^2 s_0^2 - \mu_q^2 G_{0\psi} G_{0\chi}\right) \\
& \times \left(\widehat{(p+q)}^2 G_{0\psi}^2 + G_{0\psi}^2 G_{0\chi}^2 s_0^2 - \mu_{p+q}^2 G_{0\psi} G_{0\chi}\right) s_0^2 \\
& + \left(\bar{q}^2 + \mu_q^2 - G_{0\psi} G_{0\chi} s_0^2\right)\left(\widehat{(p+q)}^2 + \mu_{p+q}^2 - G_{0\psi} G_{0\chi} s_0^2\right) G_{0\psi} G_{0\chi} \mu_q \mu_{p+q} \\
& - \left(\bar{q}^2 + \mu_q^2 + G_{0\chi}^2 s_0^2\right)\left(\widehat{(p+q)}^2 + \mu_{p+q}^2 + G_{0\chi}^2 s_0^2\right) G_{0\psi}^2 \bar{q} \cdot \widehat{p+q} \\
& - \mu_q \mu_{p+q} \left(G_{0\psi} + G_{0\chi}\right)^2 G_{0\psi} G_{0\chi} s_0^2 \bar{q} \cdot \widehat{p+q} + (\psi \leftrightarrow \chi) \Big\} .
\end{aligned}
\tag{68}
$$

This expression is infrared singular at $p = 0$ due to the massless π-propagator in the sixth term. Therefore the renormalized sigma mass has to be defined at non-zero momentum. We choose to consider the physical sigma mass m_σ, which is given by the complex pole of the propagator through

$$
\Gamma_\sigma\left(i m_\sigma + \tfrac{1}{2}\gamma_\sigma, 0, 0, 0\right) = 0 . \tag{69}
$$

At tree level its value is

$$
m_\sigma = 2 \log\left(m_0/2 + \sqrt{1 + m_0^2/4}\right) . \tag{70}
$$

The one-loop correction can be derived straightforwardly from eq. (68) but is too lengthy to be displayed here.

In the infinite-volume limit the vacuum expectation value of the scalar field $v = \langle \phi \rangle$ is related to the vacuum expectation value of the shifted σ-field by

$$
\sqrt{2\kappa}\, v = s_0 + \langle \sigma \rangle . \tag{71}
$$

In perturbation theory $\langle\sigma\rangle$ is given by the sum of tadpole diagrams, which in the one-loop approximation yields

$$\langle\sigma\rangle = -s_0 \frac{g_0}{2m_0^2} \int_q \left[(\hat{q}^2 + m_0^2)^{-1} + \tfrac{1}{3}(\hat{q}^2)^{-1} \right]$$

$$+ s_0 \frac{8}{m_0^2} \int_q \tilde{D}(q)^{-1} \left\{ \bar{q}^2 \left(G_{0\psi}^2 + G_{0\chi}^2 \right) - 2\mu_q^2 G_{0\psi} G_{0\chi} + 2G_{0\psi}^2 G_{0\chi}^2 s_0^2 \right\}. \quad (72)$$

Next we come to the fermion propagator. Let a and b be indices which assume values ψ and χ. Then the inverse fermion propagator matrix in one-loop order is

$$-\frac{1}{2K} \Gamma_{ab}^{(0,2)}(p) = \tilde{W}_{ab}(p) + \delta_{ab} G_{0a} \langle\sigma\rangle$$

$$- \left\{ G_{0a} G_{0b} \int_q \left[\widetilde{(p-q)}^2 + m_0^2 \right]^{-1} \tilde{W}_{ab}^{-1}(q) + (m_0 \to 0, s_0 \to -s_0) \right\}. \quad (73)$$

From this expression the matrices M and N, which describe the behaviour of the inverse propagator near $p = 0$ according to eq. (29), can be derived. The result is

$$\frac{1}{2K} m_1 = G_{0\psi}(s_0 + \langle\sigma\rangle)$$

$$\times \left\{ 1 - G_{0\psi} \int_q \left[(\hat{q}^2 + m_0^2)^{-1} - (\hat{q}^2)^{-1} \right] \tilde{D}(q)^{-1} \left[(\bar{q}^2 + G_{0\chi}^2 s_0^2) G_{0\psi} - \mu_q^2 G_{0\chi} \right] \right\}, \quad (74)$$

$$\frac{1}{2K} m_2 = \text{ditto with } (\psi \leftrightarrow \chi), \quad (75)$$

$$\frac{1}{2K} m = \mu_0 - G_{0\psi} G_{0\chi} \int_q \left[(\hat{q}^2 + m_0^2)^{-1} + (\hat{q}^2)^{-1} \right] \tilde{D}(q)^{-1} (\bar{q}^2 + \mu_q^2 - G_{0\psi} G_{0\chi} s_0^2) \mu_q, \quad (76)$$

$$\frac{1}{2K} n_1 = 1 + \tfrac{1}{2} G_{0\psi}^2 \int_q \left[(\hat{q}^2 + m_0^2)^{-2} + (\hat{q}^2)^{-2} \right] \tilde{D}(q)^{-1} (\bar{q}^2 + \mu_q^2 + G_{0\chi}^2 s_0^2) \bar{q}^2, \quad (77)$$

$$\frac{1}{2K} n_2 = \text{ditto with } (\psi \leftrightarrow \chi), \quad (78)$$

$$\frac{1}{2K} n = -\tfrac{1}{2} G_{0\psi} G_{0\chi} (G_{0\psi} + G_{0\chi}) s_0 \int_q \left[(\hat{q}^2 + m_0^2)^{-2} - (\hat{q}^2)^{-2} \right] \tilde{D}(q)^{-1} \bar{q}^2 \mu_q. \quad (79)$$

The diagonalization of these matrices leads to the definition of the fermionic wave-function renormalization factors, renormalized Yukawa couplings and fermion masses as explained in the previous section. The one-loop expressions for these quantities are straightforwardly obtained by inserting the expressions for M and N above into eqs. (34)–(37).

The perturbative relations between bare masses and couplings and their corresponding renormalized counterparts discussed above can be inverted in order to express the bare quantities in terms of the renormalized ones. If these expressions are substituted into the expansions of other physical quantities, say higher vertex functions, renormalized perturbation theory is obtained, where divergencies are eliminated. A particular example are perturbative finite-size effects. The finite lattice-size dependence of various quantities can be obtained from the formulae above in the same way as in ref. [11] and can be evaluated numerically.

Particularly interesting for the investigation of spontaneous symmetry breaking is the effective potential for the scalar field. For constant fields ϕ the coefficients of its power series expansion (if they exist) are the zero momentum vertex functions:

$$U(\phi) = -\sum_{N=2}^{\infty} \frac{1}{N!} \Gamma^{(N,0)}_{i_1,\ldots,i_N}(0,\ldots,0)\phi_{i_1}\ldots\phi_{i_N}. \tag{80}$$

As is well known the effective potential can be obtained by perturbation theory around the point $\phi = 0$ in the case of a spontaneous breakdown of symmetry as well. In this case the Feynman rules of the symmetric phase [11] have to be used, where in our case m_0^2 has to be replaced by $-m_0^2/2$ according to eq. (40).

In the one-loop approximation the effective potential is

$$U(\phi) = -\frac{m_0^2}{2}|\phi_0|^2 + \frac{g_0}{6}|\phi_0|^4 + \tfrac{1}{2}\operatorname{Tr}\log D - \operatorname{Tr}\log Q - \operatorname{Tr}\log Q^+, \tag{81}$$

where

$$D_{xy} = \left.\frac{\delta^2 S}{2\delta\phi_0(x)\delta\phi_0(y)}\right|_{\phi_0=\text{const.}} \tag{82}$$

and Q is the fermion matrix of eq. (3). The matrix

$$D_{xy} = \left(-\partial_\mu\partial_\mu - \frac{m_0^2}{2} + \frac{g_0}{3}|\phi_0|^2\right)\delta_{xy}\begin{pmatrix}1 & 0\\ 0 & 1\end{pmatrix} + \frac{g_0}{3}\delta_{xy}\begin{pmatrix}\phi_{01}^2 & \phi_{01}\phi_{02}\\ \phi_{01}\phi_{02} & \phi_{02}^2\end{pmatrix} \tag{83}$$

is easily diagonalized and yields

$$\tfrac{1}{2}\,\mathrm{Tr}\log D = \frac{1}{2}\int_q \left\{ \log\left(\hat{q}^2 - \frac{m_0^2}{2} + g_0|\phi_0|^2 \right) + \log\left(\hat{q}^2 - \frac{m_0^2}{2} + \frac{g_0}{3}|\phi_0|^2 \right) \right\}. \quad (84)$$

We write the fermion matrix as

$$\frac{Q}{2K} = W + V_i \phi_{0i}, \quad (85)$$

where W is as in eq. (57) but without the s_0-term. For the fermionic contribution we obtain

$$\begin{aligned} 2\,\mathrm{Tr}\log Q &= 2\,\mathrm{Tr}\log(1 + W^{-1}V_i\phi_{0i}) + \text{const.} \\ &= \mathrm{Tr}\log(1 - W^{-1}V_i\phi_{0i}W^{-1}V_k\phi_{0k}) \\ &= \int_q \mathrm{tr}\log\left\{ \left(\bar{q}^2 + \mu_q^2\right)^2 - 2|\phi_0|^2 \right. \\ &\qquad \left. \times \begin{pmatrix} -\hat{q}^2 G_{0\psi}^2 + \mu_q^2 G_{0\psi}G_{0\chi} & -i\gamma\cdot\bar{q}\,\mu_q G_{0\chi}(G_{0\psi} + G_{0\chi}) \\ -i\gamma\cdot\bar{q}\,\mu_q G_{0\psi}(G_{0\psi} + G_{0\chi}) & -\hat{q}^2 G_{0\chi}^2 + \mu_q^2 G_{0\psi}G_{0\chi} \end{pmatrix} \right\} \\ &= 4\int_q \left\{ \left(\bar{q}^2 + \mu_q^2 - 2G_{0\psi}G_{0\chi}|\phi_0|^2\right)^2 + 2\bar{q}^2(G_{0\psi} + G_{0\chi})^2|\phi_0|^2 \right\}. \end{aligned} \quad (86)$$

The vacuum expectation value of the scalar field is determined by the minimum of the effective potential. Through differentiation of the one-loop expression for $U(\phi)$ the result (72) can be confirmed.

Expressing the bare fields and parameters in terms of the renormalized ones in the effective potential yields a renormalized potential $U_R(\phi_R)$ which is free of UV-divergencies. The infrared singularities of the scalar propagator mentioned above show up if the effective potential is expanded around its minimum. We obtain a contribution of the form

$$\frac{1}{64\pi^2}\left(\tfrac{1}{3}g_R v_R \sigma_R + \frac{g_R}{6}\left(\sigma_R^2 + \pi_R^2\right) \right)^2 \log\left| \left(2 g_R v_R \sigma_R + g_R(\sigma_R + \pi_R)^2\right)/3m_\sigma^2 \right|, \quad (87)$$

which cannot be expanded in powers of the shifted fields.

For large $|\phi_R|$ the leading term in the one-loop effective potential is the logarithmic contribution

$$B|\phi_R|^4 \log \frac{|\phi_R|^2}{v_R^2} \quad (88)$$

with

$$B = \frac{1}{64\pi^2}\left(\frac{10}{9}g_R^2 - 32G_{R\psi}^4 - 32G_{R\chi}^4\right). \tag{89}$$

It reveals the breakdown of the one-loop approximation for large fields and makes the summation of the leading logarithms with the help of the renormalization group necessary [16]. This leads to the consideration of "vacuum stability" bounds, which are discussed in sect. 6.

5. Mirror-symmetry breaking: heavy mirror fermions

The vacuum expectation value of the scalar field induces non-zero diagonal elements in the fermion mass matrix (35). Therefore the physical fermion states are mixtures of the (ψ, χ)-states with a mixing angle α_R and with two, in general different, mas eigenvalues μ_{1R} and μ_{2R}. From the point of view of chiral Yukawa models the most interesting situation is zero mixing: $\alpha_R = 0$. In this case a $U(1)_L$ gauge field has a pure $V-A$ coupling to one of the states (and pure $V+A$ coupling to the other). In the present paper we shall only be interested in $\alpha_R \simeq 0$, which can be achieved, for instance, by an appropriate tuning of the fermion hopping parameter K. (Since $\alpha_R = 0$ corresponds to zero off-diagonal fermion mass $\mu_R = 0$, it is natural to tune by K but, of course, one can in general speak about the four-parameter subspace defined by $\alpha_R = 0$ in the space of five bare parameters $\{\kappa, K, \lambda, G_\psi, G_\chi\}$.)

For zero mixing the two fermion masses are given by $G_{R\psi}v_R$ and $G_{R\chi}v_R$, respectively. Therefore a heavy mirror fermion corresponds to a large value of the renormalized Yukawa-coupling $G_{R\chi}$. If there were similar upper limits for renormalized Yukawa couplings as in pure scalar ϕ^4 models for the renormalized quartic scalar coupling (see, for instance, refs. [26, 27]), then it would be impossible to make the mirror fermion really heavy. Nevertheless, we have seen in the symmetric phase that the renormalized Yukawa couplings can be rather large [11]. It is expected on general grounds that the qualitative features of renormalization are the same in both phases. Therefore in the broken phase the mirror fermion can presumably be rather heavy. It is also possible that there is a non-trivial fixed point for the Yukawa couplings (which would correspond to the qualitative behaviour of the two-loop β-functions). In this case there is no upper limit on the renormalized Yukawa couplings and the mirror fermion can be infinitely heavy. This opens up a new possibility for removing the mirror fermion from the physical spectrum. Therefore, after knowing the results in the symmetric phase, we changed our strategy for the numerical simulations in the broken phase. Namely originally we were planning to follow the suggestion of ref. [15] and to try to decouple the mirror fermion by tuning it to zero mass and zero mixing. On the other hand the

decoupling with a heavy mass is more natural and it can also immediately be extended to the case of weak gauge fields. Thus in the present paper we try to tune the mass of the mirror fermion to large values by increasing G_χ.

As a consequence both bare Yukawa couplings G_ψ and G_χ have to be non-zero. A few test runs with $G_\psi G_\chi \neq 0$ showed, both in the symmetric and broken phases, that compared to $G_\psi G_\chi = 0$ the doubler masses are decreasing for $G_\psi G_\chi > 0$ and increasing for $G_\psi G_\chi < 0$. Since we want to make the doublers as heavy as possible, in the following we always consider G_ψ positive and G_χ negative. Note that an overall sign of the Yukawa couplings can be compensated by the transformation $\phi_x \to -\phi_x$, but the relative sign of G_ψ and G_χ cannot be transformed away. The signs of the renormalized Yukawa couplings usually remain the same as those of the bare ones. This means that we get a negative renormalized fermion mass for one of the states. The sign of the fermion mass, however, is insignificant, because one can change it by an appropriate γ_5-transformation (see ref. [11]). It is remarkable that the opposite signs of G_ψ and G_χ are also preferred by the site-reflection positivity condition in eq. (17) in the sense that in the overwhelming part of the region $|G_\psi + G_\chi| < 2(1 - 6|K|)$ the signs of G_ψ and G_χ are opposite.

The Monte Carlo simulations were performed on $4^3 \times 8$, $4^3 \times 16$ and $6^3 \times 16$ lattices with periodic boundary conditions in the space directions. In the (longest) time direction periodic boundary conditions were taken for the scalar field and antiperiodic ones for the fermions. The larger time extension is favourable for the definition of fermionic renormalized quantities because of the smaller value of the smallest non-zero momentum in the time direction. In the molecular-dynamics step typically 15000 to 40000 trajectories per point were calculated, with a few thousand at the beginning used for equilibration. The number of leapfrog steps per trajectory was chosen randomly between 4 and 10. The step length was tuned so that the acceptance rate for the trajectories was near 75–80%. The typical average trajectory length was between 0.5 and 1.5. The necessary inversions of the fermion matrix were done by the conjugate gradient iteration, until the residuum was smaller than 10^{-8} times the length square of the input vector.

The Wilson parameter in the lattice action (1), (2) was always chosen to be $r = 1$. We have seen in the symmetric phase that the value of bare quartic coupling λ did not influence the results at all, at least within the typical statistical errors and as long as λ was within the range 0.1–10.0. This should be qualitatively similar in the broken phase, too. Therefore here we only performed numerical simulations at $\lambda = \infty$ and at almost zero λ, namely $\lambda = 10^{-4}$ and $\lambda = 10^{-6}$. (We did not choose λ to be exactly zero, in order to be sure about the convergence of the Monte Carlo process.) A summary of our data points is collected in table 1. Some global expectation values in these points are given in table 2. The results for the renormalized couplings and for the wave-function renormalization parameters, as defined in sect. 3, are included in table 3. In the present section we shall

TABLE 1

The chosen points in the parameter space and the measured renormalized masses m_L, μ_R, μ_{1R} and μ_{2R}. Statistical errors in last numerals are in parentheses. Points with labels in capital letters are at $\lambda = \infty$, others with small letters at $\lambda = 10^{-4}$ and those with a greek letter at $\lambda = 10^{-6}$

Label	$L^3 \cdot T$	G_ψ	G_χ	κ	K	m_L	μ_R	μ_{1R}	μ_{2R}
A	$4^3 \times 8$	0.1	−0.6	0.088	0.125	1.30(4)	−0.012(3)	0.2324(5)	0.983(4)
B	$4^3 \times 16$	0.1	−0.6	0.088	0.125	1.10(5)	−0.031(21)	0.2091(5)	0.945(13)
C	$6^3 \times 16$	0.1	−0.6	0.088	0.125	0.78(7)	−0.059(14)	0.194(1)	0.701(14)
D	$4^3 \times 8$	0.2	−0.6	0.080	0.127	0.99(7)	−0.049(27)	0.462(1)	0.964(8)
E	$4^3 \times 8$	0.3	−0.6	0.072	0.133	1.11(5)	−0.28(2)	0.619(2)	1.041(10)
F	$4^3 \times 8$	0.4	−0.6	0.050	0.142	1.27(6)	−0.16(11)	0.702(11)	0.968(11)
G	$4^3 \times 8$	0.5	−0.6	0.032	0.153	1.60(3)	−0.20(17)	0.856(5)	1.017(6)
H	$4^3 \times 8$	0.6	−0.6	0.030	0.155	1.59(4)	−0.8(2)	1.117(4)	1.119(5)
I	$4^3 \times 8$	0.1	−0.7	0.073	0.125	1.36(6)	−0.011(8)	0.2384(3)	1.116(10)
J	$4^3 \times 8$	0.1	−0.8	0.059	0.125	1.39(6)	−0.039(9)	0.2463(4)	1.30(2)
K	$4^3 \times 8$	0.1	−0.9	0.046	0.125	1.62(8)	−0.055(13)	0.2530(5)	1.51(2)
L	$4^3 \times 8$	0.1	−1.0	0.030	0.125	1.60(8)	−0.073(11)	0.2583(3)	1.63(2)
M	$4^3 \times 16$	0.1	−1.0	0.030	0.125	1.30(8)	−0.27(7)	0.2386(3)	1.53(6)
a	$4^3 \times 8$	0.1	−0.1	0.110	0.130	0.51(9)	0.22(4)	0.286(4)	0.286(3)
b	$4^3 \times 8$	0.1	−0.2	0.096	0.130	0.72(4)	−0.001(3)	0.286(2)	0.555(3)
c	$4^3 \times 8$	0.1	−0.3	0.081	0.130	0.90(3)	−0.001(3)	0.2656(8)	0.54(3)
d	$4^3 \times 8$	0.1	−0.4	0.065	0.130	1.14(3)	−0.007(3)	0.249(1)	0.895(6)
e	$4^3 \times 8$	0.1	−0.5	0.049	0.130	1.27(3)	−0.016(3)	0.2467(7)	1.025(6)
f	$4^3 \times 8$	0.1	−0.6	0.032	0.129	1.28(6)	−0.021(5)	0.2594(6)	1.05(2)
α	$4^3 \times 8$	0.1	−0.6	0.032	0.129	1.32(6)	−0.025(6)	0.2610(7)	1.06(2)
β	$6^3 \times 16$	0.1	−0.6	0.032	0.129	0.73(7)	−0.11(2)	0.207(1)	0.65(2)

concentrate on the $\lambda = \infty$ points. The data at very small λ will be discussed in the next section in connection with the vacuum stability bound.

An important question to be investigated is whether the doubler masses are kept large by the off-diagonal Wilson term, as is suggested by lattice perturbation theory and has been shown by the numerical simulations in the symmetric phase [11]. A slight complication in the broken phase is the mixing and the mass splitting of the doublers due to the scalar vacuum expectation value. In an unfavourable situation the mixing could push down one of the states with respect to the mean value. This does not happen if the off-diagonal terms in the mass matrix of the doublers are sufficiently dominating, because then the two masses are nearly degenerate. The numerical data show, that for the chosen points with $G_\psi G_\chi < 0$ all the doubler masses remain above 1.7–1.8 in lattice units (see fig. 1), and the mixing angles are always roughly about $\pi/4$. A closer look at the results shows that the splitting of the doubler masses is sensitive to the quality of the tuning to $\alpha_R = 0$ at the zero corner. If the mixing at the zero corner is closer to zero, then the splitting of the doublers is usually smaller.

TABLE 2

Some global expectation values in the points with label defined in table 1. l is the normalized link variable defined in eq. (120) of ref. [11]. $|\phi|$ denotes the absolute value of the average scalar field, v_R is the renormalized average scalar field and α_R is the mixing angle. The other notations are self-explaining. Statistical errors in last numerals are given in parentheses

	l	$\langle\|\phi\|\rangle$	$\langle\psi_x\bar{\psi}_x\rangle$	$\langle\chi_x\bar{\chi}_x\rangle$	v_R	α_R
A	0.244(1)	0.371(1)	0.930(6)	−0.376(3)	0.267(1)	−0.010(2)
B	0.246(2)	0.353(4)	0.91(1)	−0.356(4)	0.297(15)	−0.027(18)
C	0.205(2)	0.273(8)	0.65(2)	−0.271(7)	0.183(63)	−0.066(16)
D	0.213(2)	0.313(4)	0.779(8)	−0.395(4)	0.229(5)	−0.034(19)
E	0.231(2)	0.347(4)	0.819(8)	−0.519(5)	0.246(4)	−0.169(12)
F	0.218(1)	0.345(3)	0.814(5)	−0.624(4)	0.253(5)	−0.098(75)
G	0.248(1)	0.405(3)	0.922(6)	−0.819(5)	0.299(8)	−0.115(97)
H	0.2718(6)	0.431(1)	0.937(2)	−0.936(2)	0.304(4)	−0.4(2)
I	0.233(3)	0.360(5)	1.020(6)	−0.376(2)	0.262(7)	−0.0084(43)
J	0.238(2)	0.375(4)	1.182(9)	−0.400(3)	0.274(7)	−0.025(6)
K	0.246(2)	0.393(3)	1.36(1)	−0.422(3)	0.296(7)	−0.031(5)
L	0.239(1)	0.389(3)	1.461(9)	−0.426(2)	0.288(7)	−0.039(6)
M	0.241(1)	0.374(3)	1.43(1)	−0.408(4)	0.33(2)	−0.16(5)
a	0.448(4)	0.780(8)	0.464(4)	−0.463(5)	0.425(5)	0.44(10)
b	0.411(2)	0.752(4)	0.709(3)	−0.513(2)	0.406(4)	−0.002(3)
c	0.356(1)	0.674(2)	0.859(2)	−0.501(1)	0.363(4)	−0.001(3)
d	0.301(2)	0.594(3)	0.946(4)	−0.472(2)	0.322(4)	−0.006(2)
e	0.2592(9)	0.538(2)	1.019(4)	−0.447(2)	0.293(4)	−0.012(3)
f	0.203(2)	0.444(4)	0.982(7)	−0.384(3)	0.259(5)	−0.016(4)
α	0.206(2)	0.448(4)	0.989(9)	−0.387(4)	0.254(7)	−0.019(5)
β	0.160(2)	0.269(9)	0.58(2)	−0.237(8)	0.18(2)	−0.13(2)

The second question in the broken phase is whether the mirror fermion can be made sufficiently heavy by choosing G_χ large. Also here the first general observation is that this is rather sensitive to the smallness of the mixing angle α_R. For fixed values of the bare Yukawa couplings, the smaller α_R, the larger can the mass splitting of the dominant ψ- and χ-states be. The opposite of this statement sounds more familiar: for large mass splittings the mixing has to be small. The sensitivity of the mass values of the tuning of α_R is also a difficulty because, unfortunately, the fluctuations of α_R during the Monte Carlo process turned out to be large. Therefore the tuning of α_R requires long runs, especially at large bare Yukawa couplings. The measured masses of the fermion and mirror fermion on a $4^3 \times 8$ lattice are shown in figs. 2 and 3. According to fig. 2 the mirror fermion mass can be kept near 1 for decreasing fermion mass. The opposite is done in fig. 3: for fixed small fermion mass the mirror fermion mass is increased beyond 1. The maximum value of the mirror fermion mass in the last point at ($G_\psi = 0.1$; $G_\chi = -1.0$) is about 1.6–1.7, which is practically the same as the lowest doubler mass.

The masses in the tables and figures were obtained, according to the formulae in sect. 3, from the behaviour of the propagator at the lowest timelike momenta. An

TABLE 3
Renormalized couplings, Z-factors and the angle ζ defined in eq. (33) in the points with label defined in table 1. Statistical errors in the last numerals are given in parentheses

	g_R	$G_{R\psi}$	$G_{R\chi}$	Z_L	Z_T	Z_ψ	Z_χ	ζ
A	71(5)	0.87(2)	−3.68(11)	2.96(12)	1.93(9)	1.077(7)	3.28(2)	0.26(1)
B	42(7)	0.70(4)	−3.17(17)	2.71(13)	1.41(15)	2.15(1)	3.47(5)	0.24(2)
C	54(12)	1.04(13)	−3.82(35)	2.82(16)	2.22(37)	1.96(2)	3.21(3)	0.35(2)
D	57(4)	2.01(4)	−4.20(7)	2.73(9)	1.86(5)	2.30(1)	3.17(3)	0.40(3)
E	60(4)	2.33(6)	−4.05(8)	2.66(14)	2.03(8)	2.66(1)	3.09(3)	0.48(2)
F	75(4)	2.7(3)	−3.77(28)	2.89(9)	1.87(6)	2.66(2)	2.86(3)	0.33(9)
G	87(8)	2.67(9)	−3.21(15)	2.91(9)	1.84(7)	2.62(2)	2.73(3)	0.20(10)
H	82(4)	2.5(3)	−2.5(3)	2.63(7)	2.01(5)	2.75(2)	2.77(2)	0.5(2)
I	81(6)	0.91(2)	−4.26(12)	3.08(12)	1.89(10)	1.121(5)	3.31(3)	0.26(7)
J	77(6)	0.89(2)	−4.73(13)	2.77(11)	1.87(7)	1.171(5)	3.34(5)	0.26(8)
K	90(7)	0.85(2)	−5.09(13)	3.1(1)	1.76(7)	1.21(5)	3.35(4)	0.25(9)
L	93(9)	0.87(2)	−5.65(13)	2.54(14)	1.82(7)	1.247(4)	3.27(3)	0.262(9)
M	46(5)	0.59(11)	−4.5(2)	2.30(12)	1.27(12)	2.38(3)	3.15(9)	0.36(5)
a	4.2(4)	0.43(6)	−0.43(6)	3.61(7)	3.37(5)	1.34(2)	1.34(2)	−0.49(7)
b	9.4(5)	0.703(5)	−1.365(12)	4.28(8)	3.42(5)	1.37(1)	2.54(1)	0.032(3)
c	18.3(8)	0.733(7)	−2.08(2)	4.71(9)	3.45(6)	1.248(4)	2.96(2)	0.081(4)
d	38(2)	0.774(7)	−2.78(3)	4.9(1)	3.41(5)	1.140(7)	3.09(2)	0.133(3)
e	57(3)	0.84(2)	−3.50(5)	5.5(2)	3.38(8)	1.127(5)	3.16(2)	0.179(4)
f	72(6)	1.00(2)	−4.05(8)	5.4(2)	2.93(9)	1.218(6)	3.14(3)	0.264(6)
α	80(5)	1.03(3)	−4.18(9)	5.7(3)	3.1(2)	1.232(6)	3.13(4)	0.267(7)
β	46(9)	1.09(9)	−3.6(3)	4.3(3)	2.3(3)	2.01(2)	3.07(5)	0.47(3)

alternative possibility is to use cosh and sinh fits to the appropriate matrix elements of the fermion propagator. This is particularly simple for degenerate fermion masses (e.g. at $G_\psi = -G_\chi$). Therefore, as a check, the fermion mass at $G_\psi = -G_\chi = 0.6$ was determined also from such fits. A cosh fit to matrix elements like $\langle \psi_L \gamma_4 \bar{\chi}_L \rangle$ gives $\mu_{1R} = \mu_{2R} = 1.05(2)$. A sinh fit to matrix elements like $\langle \psi_L \bar{\chi}_R \rangle$ gives $\mu_{1R} = \mu_{2R} = 1.02(4)$. This has to be compared with the values in table 1. $\mu_{1R} = 1.117(4)$, $\mu_{2R} = 1.119(5)$. The agreement is reasonably good, but the fits give 5–10% lower values.

It cannot be expected that on our $4^3 \times 8$ lattice the finite-size effects are small. A detailed study on large lattices has to be left for later studies. In the present paper we only report on a first look at the lattice-size dependence. Due to the small masses one can expect that for fixed space volumes still larger time extensions are needed. In order to see the effect of finite T, we increased it to $T = 16$ in the points at $(G_\psi = 0.1;\ G_\chi = -0.6)$ and $(G_\psi = 0.1;\ G_\chi = -1.0)$. Most quantities change only little, but the Higgs-boson mass and especially the renormalized quartic coupling becomes substantially smaller. An even larger change of these quantities is observed if in the $(G_\psi = 0.1;\ G_\chi = -0.6)$ point the spatial lattice size is increased to 6^3. The change of the fermionic quantities, however, remains moder-

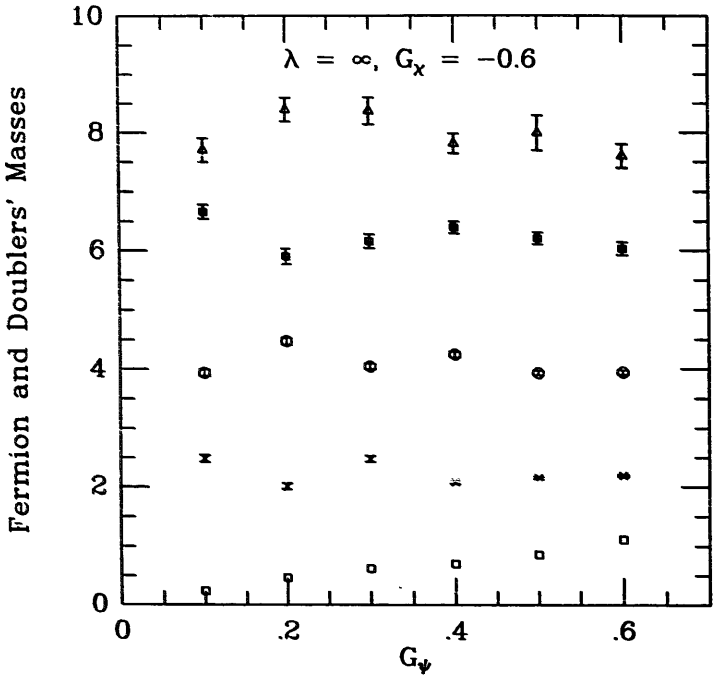

Fig. 1. The fermion masses at different corners of the Brillouin zone on the $4^3 \times 8$ lattice at $\lambda = \infty$ and $G_\chi = -0.6$ as a function of the bare Yukawa coupling G_ψ. The masses increase monotonously with the increasing number of π-values in the lattice momentum.

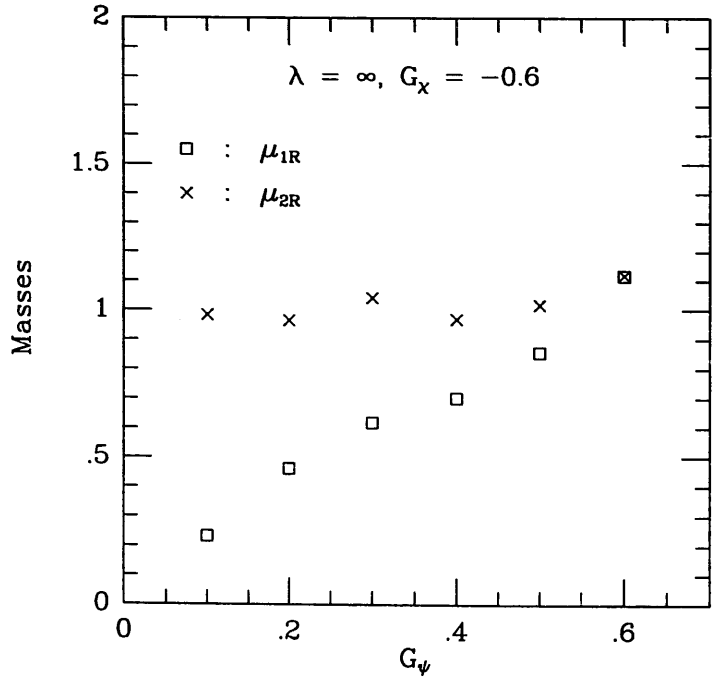

Fig. 2. Masses of the fermion and mirror-fermion measured on the $4^3 \times 8$ lattice at $\lambda = \infty$ and $G_\chi = -0.6$ are plotted as a function of G_ψ. Squares denote the fermion masses and crosses are for the mirror-fermion masses. Errors are comparable to the size of the symbols.

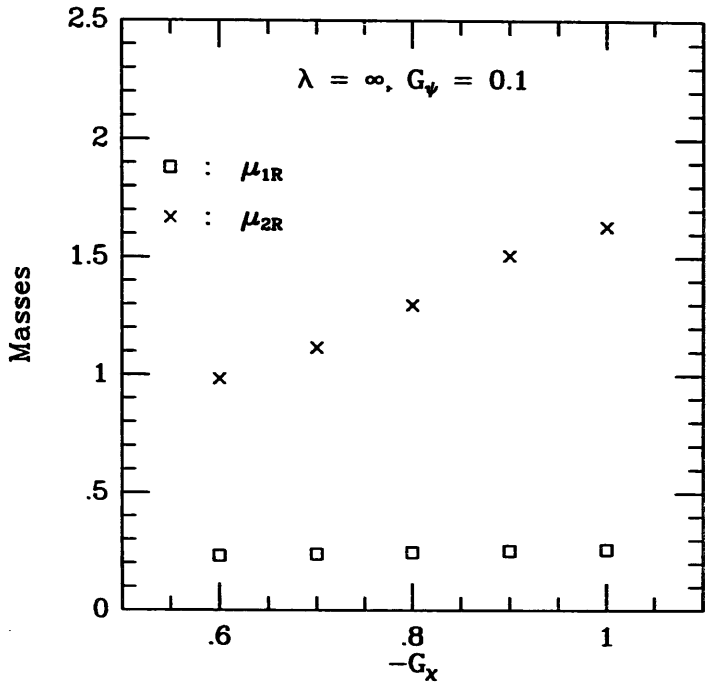

Fig. 3. The same plot as fig. 2 except that masses are now plotted as a function of $-G_\chi$ at $G_\psi = 0.1$.

ate. In particular, the renormalized Yukawa coupling of the mirror fermion is similarly large as on the smaller lattice, in such a way that the ratios $G_{R\chi}/G_{R\psi}$ and μ_{2R}/μ_{1R} are almost the same on the $4^3 \times 8$, $4^3 \times 16$ and $6^3 \times 16$ lattice. It is clear, however, that the $4^3 \times 8$ lattice is only indicating the qualitative behaviour. For quantitative results considerably larger lattices are needed.

6. The "vacuum stability" bound on the Higgs mass

As has been mentioned at the end of sect. 4 the perturbative expansion of the effective potential breaks down for large values of the scalar field ϕ. This is due to the appearance of logarithms of the field in the coefficient of the quartic term. In the literature this situation has been dealt with by a summation of the leading logs by means of the renormalization group [16]. The coefficient of the ϕ^4-term is then equal to the running quartic coupling at a scale which is given by the value of the field. Given some values of the renormalized couplings g_R, $G_{R\psi}$ and $G_{R\chi}$ at the physical scale, the renormalization group equations can be integrated upwards to some high scale to yield the corresponding quartic coupling. An important qualitative feature of the Callan–Symanzik β-function of the quartic scalar coupling is that in some region, namely at small couplings and large ratios $G_{R\psi}/g_R$ and/or $G_{R\chi}/g_R$, it is negative. Consequently it may happen that for large fields one ends up with a running coupling which is negative, and the effective potential appears to bend over to large negative values. This situation has been called "vacuum

instability" and the corresponding values of the renormalized couplings, for which it occurs, are excluded from the allowed region. This implies the "vacuum stability" bound on the renormalized quartic coupling (that is, on the Higgs-boson mass) [16].

Now the question poses itself, what is the meaning of vacuum stability in the framework of the lattice regularized theory. Here the effective potential is a well-defined quantity, which is known to be convex due to a theorem of Symanzik [29]. Consequently it cannot possibly bend over to negative values for large fields because it is finite (e.g. zero by convention) at its minimum.

The resolution of this apparent paradox is related to the fact that the running coupling at the cut-off scale is essentially equal to the bare coupling. In order that the theory be well defined the bare coupling λ has to be positive. The renormalization group flow may now be followed downwards from the cut-off scale to the physical scale, where the renormalized couplings are defined. Those values of the renormalized couplings that can be reached starting from any positive value of the bare coupling form the physical admissible region. Those outside would not correspond to any positive bare λ and cannot be realized for the given cut-off. In particular the boundary corresponding to $\lambda = 0$ yields the vacuum stability bound.

To conclude, a non-perturbative formulation of the vacuum stability bound is the requirement of a positive bare quartic coupling λ. The problem is not primarily the large field behavior of the effective potential. Furthermore the cut-off plays an important rôle, which has not always been emphasized in the literature.

The exact effective potential and exact β-functions are, of course, not known. Therefore one has to rely on some approximations like perturbation theory or numerical simulations. Without knowing the qualitative behaviour of the β-functions it is impossible to derive the vacuum stability bound. In particular, the qualitative discussion is different in case of a trivial continuum limit, which is qualitatively represented by the 1-loop β-functions, or if a non-trivial fixed point at non-zero couplings exists, as suggested by the qualitative features of the 2-loop approximation. (For the explicit expressions of the β-functions up to 2-loop order see sect. 3 of ref. [11].) Since the qualitative behaviour of the β-functions is not yet known, for the moment the vacuum stability bound can only be discussed if some scenario is assumed for the β-functions.

Later on one can, of course, obtain information about the β-functions from numerical simulations by studying the cut-off dependence of the allowed values of renormalized Yukawa and quartic couplings. Before going into the discussion of the vacuum stability bound let us mention three possible alternative scenarios. The allowed region A in the space of renormalized couplings can be mapped out by studying the λ-dependence of $G_{R\psi}, G_{R\chi}, g_R$ for every bare Yukawa couplings within the broken phase near the gaussian fixed point. The region A will, in general, depend on the cut-off, which can be defined, for instance, by the value of the Higgs mass in lattice units. The first possibility corresponding to a trivial

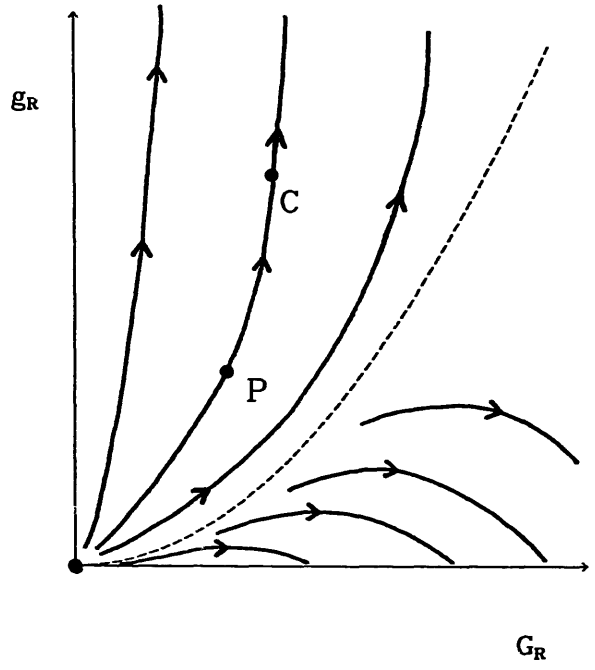

Fig. 4. The qualitative behaviour of the renormalization group flows as indicated by the 1-loop β-functions is depicted. The arrows on the flow lines are pointing in the direction of increasing energy scale. The dashed line separates two regions where the RG flows are going to positive and negative infinite values of the scalar quartic coupling respectively, and therefore gives us the lower bound on the Higgs mass if we require that the vacuum of our model be stable. In the figure, G_R means $G_{R\psi}$. We set $G_{R\chi} = 0$ or $-G_{R\psi}$. The qualitative feature of the flow lines is the same for both cases.

continuum limit is that for increasing cut-off A is shrinking to the origin $G_{R\psi} = G_{R\chi} = g_R = 0$. Another possibility is that, maybe after some shrinking for low cut-offs, the region A starts to expand and fills a 3-dimensional part of the $(G_{R\psi}, G_{R\chi}, g_R)$-space (or even the whole space) for infinite cut-off. In this case the continuum limit is non-trivial. A third possibility is that at infinite cut-off region A becomes a lower-dimensional subset, say, a surface. In this case the continuum theory is again non-trivial but the quartic coupling is a function of the Yukawa couplings. In other words, for given Yukawa couplings the lower and upper limit on the renormalized quartic coupling coincide.

Returning to the discussion of the vacuum stability lower bound, let us first assume that the continuum limit is trivial and the 1-loop β-functions are qualitatively correct (small scale breaking corrections to the β-functions will always be neglected here). In this case the renormalization flow of the coupling is as shown by fig. 4. (For simplicity only one Yukawa coupling is considered. For instance, one can imagine that $G_R \equiv G_{R\psi}$ and $G_{R\chi} = 0$ or $G_R \equiv G_{R\psi} = -G_{R\chi}$, which are renormalization group invariant relations.) The renormalized couplings at the physical scale (e.g. point P of the figure) are connected to the bare couplings along a flow line (point C on the figure). The length of the flow line connecting P and C

depends, of course, on the scale ratio at P and C. For a given scale ratio, i.e. for a given physical mass in lattice units, one can put the point C on the positive G_R axis where $g_R = 0$. The set of corresponding points P defines a curve, which is the vacuum stability bound for the given ratio of cut-off to physical mass. Namely, if one wanted to go with P along the flow line closer to the $g_R = 0$ axis, then the corresponding point C would have a negative bare quartic coupling, and the lattice action would become unstable. Saying it differently, since the 1-loop contribution of the fermion loop to the quartic coupling (at given bare couplings) is positive, it can happen that the bare quartic coupling needed for some combination of renormalized couplings is negative. (Note that here we refer to the true 1-loop contribution, not to its leading log at large fields.) It is clear from the figure, that for very large scale differences the lower limit implied by the requirement of stability tends to the separatrix of the flow to $g_R = \infty$ and $g_R = -\infty$. Of course, in case of a trivial continuum limit one has to take into account also the cut-off dependent upper limit on the renormalized couplings (see, for instance, fig. 2a in ref. [11]). The numerical evaluation shows, that the allowed region in the (G_R, g_R)-plane is bounded by the upper limit for g_R and by the vacuum stability bound. Note that in the literature the effect of weak gauge couplings is usually also included. Therefore there is an additional small excluded pocket near zero couplings, which is due to the Weinberg–Linde bound.

The small coupling part of the vacuum stability bound curve can be obtained from lattice perturbation theory. If the cut-off is not very far from the physical scale, in such a way that the logarithm of the scale ratio is not very large, the low orders of perturbation theory give a good approximation. Using at $\lambda = 0$ the 1-loop perturbative expressions given in sect. 4, one obtains for instance in the special case $G_{R\psi} = -G_{R\chi} = G_R$

$$g_R = \frac{96 G_R^2}{v_R^2} \int_q \left(\bar{q}^2 + \left(\mu_R + \hat{q}^2/2 \right)^2 \right)^{-1} . \tag{90}$$

In fig. 5 this is plotted for the case that the cut-off is twice the fermion mass and v_R.

The qualitative picture of the vacuum stability bound in case of a non-trivial fixed point (as in the 2-loop expression) looks quite different. For instance, the flow lines crossing the $g_R = 0$ axis in the negative direction return to positive g_R's, because they go to the non-trivial fixed point F (see fig. 6 which refers to the case $G_R \equiv G_{R\psi}$, $G_{R\chi} = 0$). Therefore, points excluded by the vacuum stability bound for some scale ratio can become again allowed for a larger scale ratio, because point C goes again to positive quartic couplings. More generally, the existence of the non-trivial fixed point F implies that for large enough scale ratios between the cut-off and the physical scale there is practically no restriction on the values of the

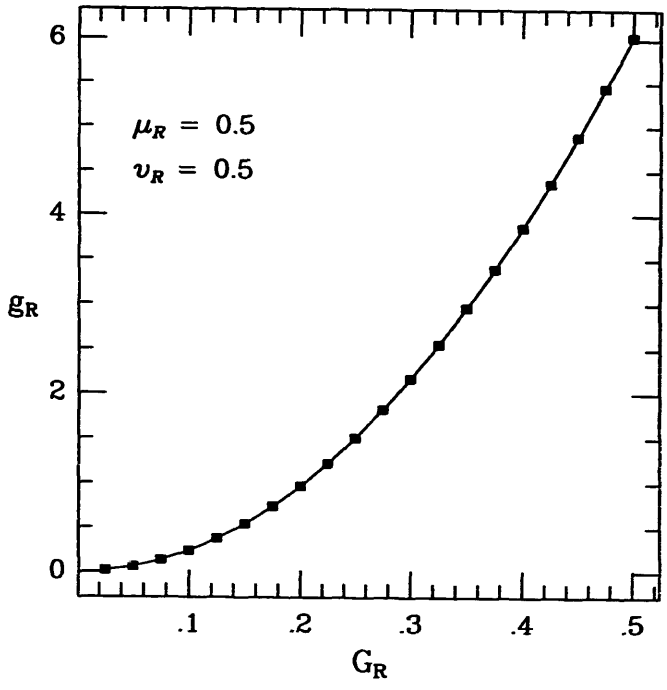

Fig. 5. The vacuum stability lower bound on the Higgs self-coupling g_R as calculated from 1-loop lattice perturbation theory is plotted for the case $G_{R\psi} = -G_{R\chi}$.

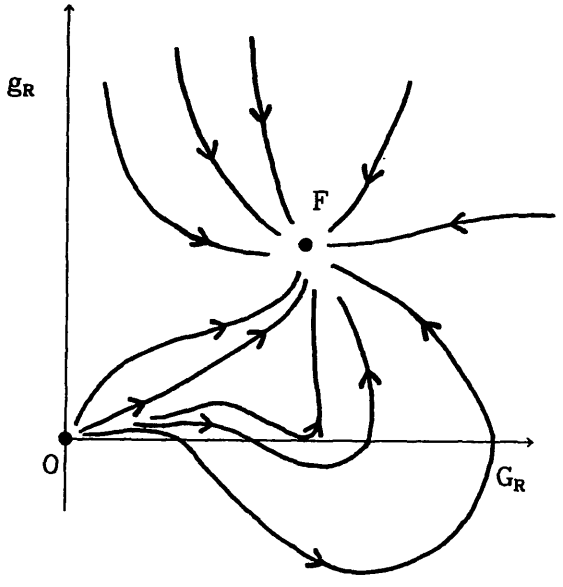

Fig. 6. The qualitative behaviour of the renormalization group flows as indicated by the 2-loop β-functions is shown. The arrows on the flow lines are pointing in the direction of increasing energy scale. We set $G_{R\chi} = 0$ in this figure. In the case where $G_{R\psi} = -G_{R\chi}$, there will be another ultraviolet attractive fixed point at negative g_R.

renormalized couplings. This is due to the fact that near F the β-functions are close to zero, and the flow can spend an arbitrarily long time there. This can be used to tune C near F such that for a large scale ratio P is an almost arbitrary point on the plane. Since, however, the β-functions are zero also at the origin O, the flow can spend a long time also there, and therefore a small region near O always remains excluded by the requirement of stability. For large scale ratios this region is, however, becoming very small. In the exact continuum limit corresponding to an infinite scale ratio every point of the plane is allowed. Note that this discussion is based on the assumption that the 2-loop β-function is correct everywhere. In reality it can happen that the non-trivial fixed point is associated to a phase transition which implies a singularity in the β-functions, too. In this case some limitations on the renormalized couplings can still arise because, for instance, some region in fig. 6 is completely absent. Another possibility is the existence of a non-physical attractive fixed point at $g_R < 0$, which occurs for instance in the 2-loop β-functions for $G_R \equiv G_{R\psi} = -G_{R\chi}$. In this case the vacuum stability bound for large cut-offs is the separatrix of the flows to the fixed points at positive and negative g_R.

This discussion shows that the qualitative features of the β-functions, in particular the existence or non-existence of a non-trivial fixed point, have to be taken into account in the numerical studies of the vacuum stability bound. Assuming that such a fixed point does not exist and that the 1-loop β-functions are qualitatively correct, a possible strategy in the numerical studies is to investigate the λ-dependence of g_R for fixed Yukawa couplings. The extreme values of the renormalized quartic coupling g_R at $\lambda = \infty$ and $\lambda = 0$ give, respectively, the upper limit implied by triviality and the lower limit implied by vacuum stability. On the basis of the results in ref. [11] one can expect that the λ-dependence of the physical quantities is weak if the bare Yukawa couplings are in the range 0.1–1.0. This is supported by the numerical data in tables 1–3 at the points with label A, f and α, which correspond to ($G_\psi = 0.1$; $G_\chi = -0.6$) but the values of λ are, respectively, $\lambda = \infty$, 10^{-4}, 10^{-6}. The obtained values of the renormalized masses and couplings are very similar in all these points. This shows that for such Yukawa couplings the lower and upper limits practically coincide. A large difference can only be expected at rather small Yukawa couplings. For instance, the perturbative vacuum stability lower bound in fig. 5 is substantially smaller than the upper limit at such small Yukawa couplings, which is practically the same as the upper limit in the pure ϕ^4 limit ($g_R \simeq 40$ in our case).

In models with fermion–mirror-fermion pairs the vacuum stability bound is, in general, a function of the two renormalized Yukawa couplings $G_{R\psi}$ and $G_{R\chi}$. As a first numerical test, we looked at the dependence of the renormalized quartic coupling on G_χ for $G_\psi = 0.1$, a fixed fermion mass of about 0.25 in lattice units and very small bare quartic couplings $\lambda = 10^{-4}$, 10^{-6} (points a–f, α and β in the tables). The results for g_R as a function of $G_{R\chi}$ are shown in fig. 7. Comparing

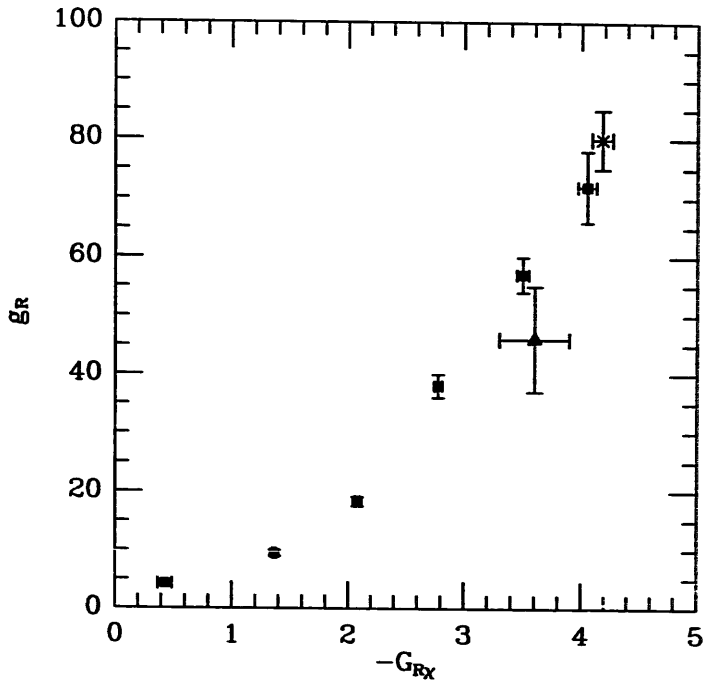

Fig. 7. Data of g_R vs. $-G_{R\chi}$ at very small values of λ at $G_\psi = 0.1$ are plotted. The point denoted by the cross is at $\lambda = 10^{-6}$ on the $4^3 \times 8$ lattice and the full triangle on the $6^3 \times 16$ lattice. Full squares are at $\lambda = 10^{-4}$ on the $4^3 \times 8$ lattice.

points f and α shows that between $\lambda = 10^{-4}$ and $\lambda = 10^{-6}$ there is practically no difference if $G_\chi = -0.6$. There might be a small difference at the other end of $G_\chi = 0.1$, where the order of magnitude of g_R is the same as the value given by perturbation theory (although this point is presumably already beyond the strict validity of the 1-loop approximation). The actual value of $g_R \simeq 70$ in point f has on the $4^3 \times 8$ lattice a large-finite size effect. The point β on a $6^3 \times 16$ lattice gives $g_R \simeq 46(9)$, a value equal within errors to the corresponding $\lambda = \infty$ point C, namely $g_R = 54(12)$, and also similar to the upper limit in the $N = 2$ pure ϕ^4 model $g_R \simeq 40$. This shows qualitatively that the vacuum stability lower bound and triviality upper bound on the Higgs mass practically coincide if the mirror-fermion mass is large. A quantitative statement of this kind needs further numerical studies on $6^3 \times 16$ and still larger (but feasible) lattices.

7. Discussion and summary

An important axiom to be fulfilled by a euclidean lattice action is the Osterwalder–Schrader reflection positivity. In sect. 2 of the present paper reflection positivity was proven in our model in a wide range of bare parameters. In particular the so-called "link-reflection positivity" was shown to be valid for every non-negative scalar hopping parameter κ. The "site-reflection positivity" could be

proven only at infinite bare quartic coupling $\lambda = \infty$ either for sufficiently small or for sufficiently large bare Yukawa coupling $G_\alpha = \frac{1}{2}(G_\psi + G_\chi)$. The vicinity of the gaussian fixed point at zero couplings, which has been numerically explored in ref. [11] and in the present paper, is at $\kappa > 0$. Therefore the link-reflection positivity implies the existence of a non-negative self-adjoint hamiltonian (and the unitarity of the S-matrix) in the corresponding quantum field theory in Minkowski space.

An important question in any lattice fermion model is the decoupling of the lattice fermion doublers in the continuum limit. The numerical simulations in both the symmetric phase [11] and in the broken phase here show that in the vicinity of the gaussian fixed point the 30 fermion doublers can be kept at rather large masses (roughly about 2 or higher in lattice units). This allows to define the desired continuum limit near the gaussian fixed point with the physical particles corresponding to the field content of the model (scalar bosons, fermion and mirror-fermion). Therefore a potentially dangerous consequence of the hopping parameter expansion at infinite bare Yukawa couplings, namely the dynamical mirror-doubling of the fermion states [30–32], does not occur in the investigated region at small or moderately large bare Yukawa couplings. In order to be able to draw qualitative conclusions from the present model for the Higgs–Yukawa sector of the Standard Model, the mirror-fermions, which were up to now not observed in nature, have to be decoupled too. The observed large values of the renormalized Yukawa couplings in the symmetric phase [11] suggest that the decoupling can be done similarly to the decoupling of the doublers, namely by large masses. The results of the numerical simulations in the broken phase show, that indeed the mirror-fermions can be made almost as heavy as the doublers. Theoretically, if a non-trivial fixed point would exist, then there were no upper limits for the renormalized couplings at all, and the mirror-fermions could be infinitely heavy. If, however, the gaussian fixed point at zero couplings would be the only fixed point, then the continuum limit would be trivial and the mirror-fermions would have to exist as "new physics" at some large energy scale. Already the present simulations together with the results of ref. [11] suggest that this scale can, indeed, be rather large, say, four times the vacuum expectation value. Nevertheless the conclusions in the present paper can only be qualitative since the lattices are small. Obviously this limit has to be made more precise in further numerical studies on larger lattices [14]. At this point it is worth to emphasize that the present phenomenology does not exclude the mirror doubling of the three fermion families even near 100 GeV [33]. Therefore the light sector of the $U(1)_L \otimes U(1)_R$ model can be as "chiral" as the standard model is known to be "chiral" phenomenologically.

A closer look at the obtained renormalized couplings in the broken phase reveals that the values are somewhat (by about 10–20%) smaller than the values in the symmetric phase at the same bare Yukawa couplings. This can, however, be due to the fact that in the broken phase the parameters are not perfectly tuned to zero renormalized fermion–mirror-fermion mixing $\alpha_R = 0$. The numerical data

clearly show a strong correlation between α_R and the renormalized Yukawa couplings $G_{R\psi}, G_{R\chi}$: the smaller α_R is, the larger are $G_{R\psi}$ and $G_{R\chi}$. Therefore it is not excluded that by an exact tuning to $\alpha_R = 0$ one would obtain very similar renormalized Yukawa couplings in both phases. If this is the case, then in the broken phase the upper limits on the fermion and/or mirror fermion masses would be rather high. The corresponding renormalized Yukawa couplings could be as high as 2–3 times the tree unitarity upper bound. This interesting question awaits further detailed numerical studies.

An interesting new feature of the Higgs–Yukawa models compared to the pure scalar ϕ^4-models is the possibility of a (cut-off dependent) lower limit on the Higgs-boson mass, the so-called "vacuum stability bound". This lower bound can be deduced from the negative β-function of the quartic scalar coupling. (For its non-perturbative definition see sect. 6.) The discussion depends substantially on the assumed fixed-point structure. In case of a non-trivial fixed point the vacuum stability bound can be very weak or not present at all. Under the more conventional assumption of a trivial continuum limit the lower bound is similar in nature to the upper bound: for fixed Yukawa couplings the largest renormalized quartic coupling is reached at infinite bare quartic coupling ($\lambda = \infty$) and the smallest at zero ($\lambda = 0$). The numerical simulations show that, in accordance with the expectations based on the perturbative renormalization group studies [16], for large Yukawa couplings the lower and upper limits are almost the same. The observed quartic coupling is almost entirely induced by the Yukawa couplings. In other words, except for very small Yukawa couplings, the renormalized quartic coupling is practically a function of the renormalized Yukawa couplings. As a consequence, if the mirror-fermions are heavy, then the Higgs boson mass is predicted within close upper and lower bounds. The simulations in two points on $6^3 \times 16$ lattices show that these upper and lower bounds at the given Yukawa couplings are within errors equal to the non-perturbative upper limit in the pure ϕ^4-model. Concerning the existence of a non-trivial fixed point the present numerical data are not conclusive. This question will be investigated in the future [14] by studying the cut-off dependence of the upper and lower bounds on the Higgs-boson mass.

We thank Martin Lüscher for helpful comments and discussions about reflection positivity. The Monte Carlo calculations for this paper have been performed on the CRAY Y-MP of HLRZ, Jülich.

References

[1] LEP Collaboration, F. Dydak, Proc. 1990 Singapore Int. Conf. on High energy physics, to be published

[2] CDF Collaboration, C. Campagnari, Proc. 1990 Singapore Int. Conf. on High energy physics, to be published

[3] D. Stephenson and A. Thornton, Phys. Lett. B212 (1988) 479;
A.M. Thornton, Phys. Lett. B227 (1989) 434

[4] A. Hasenfratz and T. Neuhaus, Phys. Lett. B220 (1989) 435;
J. Berlin, A. Hasenfratz, U.M. Heller and M. Klomfass, Phys. Lett. B249 (1990) 485
[5] Y. Shen, J. Kuti, L. Lin and P. Rossi, Nucl. Phys. B (Proc. Suppl.) 9 (1989) 99
[6] I.-H. Lee, J. Shigemitsu and R. Shrock, Nucl. Phys. B334 (1990) 265;
S. Aoki, I.-H. Lee, D. Mustaki and J. Shigemitsu, Phys. Lett. B244 (1990) 301;
S. Aoki, I.-H. Lee, J. Shigemitsu and R.E. Shrock, Phys. Lett. B243 (1990) 403
[7] W. Bock, A.K. De, K. Jansen, J. Jersák and T. Neuhaus, Phys. Lett. B231 (1989) 283;
W. Bock, A.K. De, K. Jansen, J. Jersák, T. Neuhaus and J. Smit, Nucl. Phys. B344 (1990) 207;
W. Bock and A.K. De, Phys. Lett. B245 (1990) 207
[8] M.A. Stefanov and M.M. Tsypin, Phys. Lett. B236 (1990) 344
[9] J. Smit, Nucl. Phys. B (Proc. Suppl.) 17 (1990) 3
[10] L. Lin, J.P. Ma and I. Montvay, Z. Phys. C48 (1990) 355
[11] K. Farakos, G. Koutsoumbas, L. Lin, J.P. Ma, I. Montvay and G. Münster, Nucl. Phys. B350 (1990) 474
[12] I. Montvay, Phys. Lett. B199 (1987) 89
[13] I. Montvay, Nucl. Phys. B (Proc. Suppl.) 4 (1988) 443;
I. Montvay, Phys. Lett. B205 (1988) 315
[14] L. Lin, I. Montvay, G. Münster and H. Wittig, in preparation
[15] A. Borrelli, L. Maiani, G.C. Rossi, R. Sisto and M. Testa, Phys. Lett. B221 (1989) 360
[16] M.J. Duncan, R. Philippe and M. Sher, Phys. Lett. B153 (1985) 165;
M. Sher and H.W. Zaglauer, Phys. Lett. B206 (1988) 537;
M. Sher, Phys. Rep. 179 (1989) 273;
M. Lindner, M. Sher and H.W. Zaglauer, Phys. Lett. B228 (1989) 139
[17] H. Neuberger, Phys. Rev. Lett. 60 (1988) 889; Nucl. Phys. B300 [FS22] (1988) 180;
H. Leutwyler, Nucl. Phys. B (Proc. Suppl.) 4 (1988) 248
U.M. Heller and H. Neuberger, Phys. Lett. B207 (1988) 189;
P. Hasenfratz and H. Leutwyler, Nucl. Phys. B343 (1990) 241
[18] K. Osterwalder and R. Schrader, Commun. Math. Phys. 31 (1973) 83; 42 (1975) 281
[19] P. Menotti and A. Pelissetto, Nucl. Phys. B (Proc. Suppl.) 4 (1988) 644; Commun. Math. Phys. 113 (1987) 369
[20] K. Osterwalder and E. Seiler, Ann. Phys. (N.Y.) 110 (1978) 440
[21] M. Lüscher, Commun. Math. Phys. 54 (1977) 283
[22] A. Hasenfratz, K. Jansen, J. Jersák, H.A. Kastrup, C.B. Lang, H. Leutwyler and T. Neuhaus, DESY preprint 90-077 (1990); Z. Phys. C46 (1990) 257
[23] W. Langguth, I. Montvay and P. Weisz, Nucl. Phys. B277 (1986) 11
[24] W. Langguth and I. Montvay, Z. Phys. C36 (1987) 725
[25] A. Hasenfratz and T. Neuhaus, Nucl. Phys. B297 (1988) 205
[26] L. Lin, Non-perturbative studies on the Higgs and heavy fermion sectors in the standard model, Ph.D. Thesis, UC San Diego 1989
[27] A. Hasenfratz, K. Jansen, J. Jersák, C.B. Lang, T. Neuhaus and H. Yoneyama, Nucl. Phys. B317 (1989) 81
[28] I. Montvay and P. Weisz, Nucl. Phys. B290 [FS20] (1987) 327
[29] K. Symanzik, Commun. Math. Phys. 16 (1970) 48
[30] I. Montvay, Nucl. Phys. B307 (1988) 389
[31] C.E.M. Wagner, Ph.D. Thesis, Univ. of Hamburg (1989); DESY preprint 89-083
[32] K. Farakos, G. Koutsoumbas and I. Montvay, Z. Phys. C47 (1990) 641
[33] I. Montvay, Phys. Lett. B205 (1988) 315;
F. Csikor and I. Montvay, Phys. Lett. B231 (1989) 503; Proc. Madrid Europhys. Conf. on HEP (September 1989);
F. Csikor, Z. Phys. C49 (1991) 129